HHS Public Access

Author manuscript

Biochim Biophys Acta Mol Cell Biol Lipids. Author manuscript; available in PMC 2021 February 01.

Published in final edited form as:

Biochim Biophys Acta Mol Cell Biol Lipids. 2020 February ; 1865(2): 158573. doi:10.1016/j.bbalip.2019.158573.

GPR75 RECEPTOR MEDIATES 20-HETE-SIGNALING AND METASTATIC FEATURES OF ANDROGEN-INSENSITIVE PROSTATE CANCER CELLS

Sofia Cárdenas[#1], **Cecilia Colombero**[#1], **Laura Panelo**[2], **Rambabu Dakarapu**[3], **Falck John R.**[3], **Costas Monica A.**[2], **Susana Nowicki**[1]

[1]Centro de Investigaciones Endocrinológicas “Dr. Cesar Bergada” (CEDIE) CONICET-FEI-División de Endocrinología, Hospital de Niños “Ricardo Gutierrez”, Gallo1330, C1425EFD Buenos Aires, Argentina

[2]Laboratorio de Biología Molecular y Apoptosis, Instituto de Investigaciones Médicas Alfredo Lanari, IDIM-CONICET, Facultad de Medicina, Universidad de Buenos Aires, Combatientes de Malvinas 3150, C1427ARN Buenos Aires, Argentina

[3]Department of Biochemistry, UT Southwestern Medical Center, Dallas, TX 75390

[#] These authors contributed equally to this work.

Abstract

Purpose—Recent studies have shown that 20-hydroxyeicosatetraenoic acid (20-HETE) is a key molecule in sustaining androgen-mediated prostate cancer cell survival. Thus, the aim of this study was to determine whether 20-HETE can affect the metastatic potential of androgen-insensitive prostate cancer cells, and the implication of the newly described 20-HETE receptor, GPR75, in mediating these effects.

Methods—The expression of GPR75, protein phosphorylation, actin polymerization and protein distribution were assessed by western blot and/or fluorescence microscopy. Additionally, *in vitro* assays including epithelial-mesenchymal transition (EMT), metalloproteinase-2 (MMP-2) activity, scratch wound healing, transwell invasion and soft agar colony formation were used to evaluate the effects of 20-HETE agonists/antagonists or GPR75 gene silencing on the aggressive features of PC-3 cells.

Corresponding author: Susana Nowicki Ph.D., TE +54 11 4963-5931 ext 202, nowickisusana@hotmail.com; snowicki@cedie.org.ar.

AUTHOR’S CONTRIBUTIONS

CC and SC carried out the experiments; LP and MC contributed with immunofluorescence assays; RD and JRF synthetized GPR75 agonists and antagonists; CC, SC and SN designed the experiments and analyzed the data; SN wrote the paper. All authors read and approved the final manuscript.

- *Research involving Human Participants and/or Animals*

This article does not contain any studies with human participants or animals performed by any of the authors

- *Conflict of interest*

The authors declare that they have no conflict of interest.

Results—20-HETE (0.1 nM) promoted the acquisition of a mesenchymal phenotype by increasing EMT, the release of MMP-2, cell migration and invasion, actin stress fiber formation and anchorage-independent growth. Also, 20-HETE augmented the expression of HIC-5, the phosphorylation of EGFR, NF-κB, AKT and p-38 and the intracellular redistribution of p-AKT and PKCα. These effects were impaired by GPR75 antagonism and/or silencing. Accordingly, the inhibition of 20-HETE formation with *N*-hydroxy-*N*′-(4-*n*-butyl-2-methylphenyl)formamidine (HET0016) elicited the opposite effects.

Conclusions—The present results show for the first time the involvement of the 20-HETE-GPR75 receptor in the activation of intracellular signaling known to be stimulated in cell malignant transformations leading to the differentiation of PC-3 cells towards a more aggressive phenotype. Targeting the 20-HETE/GPR75 pathway is a promising and novel approach to interfere with prostate tumor cell malignant progression.

Keywords

20-HETE; arachidonic acid metabolites; GPR75 receptor; prostate cancer; metastasis

1 INTRODUCTION

According to the classical model, the arachidonic acid (AA) cascade is bifurcated into the cyclooxygenase (COX-1 and COX-2) and lipoxygenase (LOXs) enzymatic pathways which generate, *inter alia*, prostaglandins and leukotrienes, respectively. A third, less explored pathway of the cascade is mediated by cytochrome P450 (CYP) enzymes. Several CYP4A and CYP4F enzymes generate the active signaling metabolite 20-hydroxyeicosatetraenoic acid (20-HETE) via ω-hydroxylation of AA. CYP4F2 is the most active isoform that produces 20-HETE in humans, followed by CY4A11 [1].

The finding that synthetic analogues of 20-HETE are partial or full competitive antagonists of its vasoconstrictor actions suggested the existence of a receptor for 20-HETE. Moreover, the observation that the vasoconstrictor and natriuretic actions of 20-HETE are phospholipase C (PLC) / protein kinase C (PKC) dependent, and its effects on cell migration and proliferation are associated with the activation of the Proto-Oncogene Tyrosine-Protein Kinase (c-Src) / epidermal growth factor receptor (EGFR), supported the hypothesis that these effects of 20-HETE are receptor-mediated [2]. Only recently, Garcia *et al.* demonstrated that in human endothelial cells, 20-HETE binds with high affinity and activates the G-protein coupled receptor (GPCR) GPR75, and signals via Gαq/PLC/PKC, c-Src, and mitogen-activated protein kinases (MAPK) pathways to elicit its vascular effects [3]. Early findings only showed the expression of GPR75 receptor in cells surrounding retinal arterioles and in other areas of the brain [4]. However, databases indicate a broad expression profile for the GPR75 receptor in the majority of human tissues including the brain, heart, kidney and prostate (https://www.ncbi.nlm.nih.gov/geo/tools/profileGraph.cgi?ID=GDS1096:220481_at).

Increasing reports suggest that 20-HETE can play an important role in cell growth and cancer development. *In vitro* studies show that 20-HETE induces mitogenic and angiogenic responses in several types of cancer cells, and inhibitors of the 20-HETE pathway have been

shown to reduce the growth of brain, breast and kidney tumors [5]–[7] . Moreover, other authors have reported that incubation of non-small cell lung cancer cell lines with stable agonists of 20-HETE as well as overexpression of ω-hydroxylases enhance their invasive capacity [8]. Also, inhibition of 20-HETE synthesis decreases migration and invasion in the metastatic triple negative breast cancer cell lines and reduces primary tumor growth and lung metastasis *in vivo* [9].

The expression of CYP4Z1, another ω-hydroxylase first described in normal mammary gland [10], has been suggested as a potentially reliable marker of prostate cancer prognosis utilizing biopsy specimens [11]. Besides, the urinary excretion of 20-HETE, which was significantly higher in patients with benign prostatic hypertrophy or prostate cancer than in healthy subjects, decreased to normal concentrations after removal of the prostate gland [12]. However, thus far there is complete lack of knowledge regarding the cellular actions of 20-HETE that may promote the malignant potential of prostate cancer cells.

Our laboratory has reported that 20-HETE production is key to sustain cell viability in an androgen sensitive prostate cancer cell line, primarily by prevention of apoptosis. These findings support a role for 20-HETE as a mediator in androgen driven prostate cancer cell survival [13]. Although prostate cancer tumor growth is initially dependent on androgens as documented by Huggins as early as 1941 [14], many patients eventually develop an androgen-insensitive more aggressive phenotype of prostate cancer, termed castration-resistant prostate cancer (CRPC).

Thus, in view of the increase in prostate cancer cells viability elicited by 20-HETE, considering the pro-metastatic effects of 20-HETE described in other tumor models, and in light of the recent discovery of GPR75 as the target for 20-HETE, we hypothesized that the 20-HETE-GPR75 signaling complex promotes a malignant phenotype in prostate cancer cells.

This study shows that 20-HETE increases the metastatic potential of human prostate cancer cells determined *in vitro*, such as epithelial-mesenchymal transition (EMT), migration, invasion and anchorage-independent growth in the androgen insensitive PC-3 cells. In addition, our observations show for the first time the involvement of the GPR75 receptor in the activation by 20-HETE of intracellular signaling molecules already identified to be stimulated in cellular malignant transformations. Furthermore, our results demonstrate that GPR75 receptor stimulation is necessary for the pro-metastatic actions of 20-HETE in androgen insensitive prostate cancer cells.

2 MATERIALS AND METHODS

2.1. Drugs and Reagents.

Chemicals. 20-Hhydroxyeicosatetraenoic acid (20-HETE) and N-hydroxy-N′-(4-*n*-butyl-2-methylphenyl)formamidine (HET0016), a selective inhibitor of 20-HETE synthesis, were from Cayman Chemical Company (Ann Arbor, MI, USA). N-(20-hydroxyeicosa-5[Z], 14[Z]-dienoyl)glycine (5,14-HEDGE), a synthetic analogue of 20-HETE, sodium 19(R)-hydroxyeicosa-5(Z), 14(Z)-dienoyl-L-aspartate (19-HEDE amide) and sodium ((6Z,15Z)-N-

(20-hydroxyeicosa-6(Z),15(Z)-dienoyl)aspartate) (AAA), two different antagonists of the 20-HETE receptor, were synthesized by one of the authors. Dr. J. R. Falck. All other compounds were purchased from Sigma Chemical Co (St. Louis, MO). Stock solutions of all drags were prepared in ethanol with the exception of R0318220 (water), and LY29402 and sulfasalazine (DMSO). *Antibodies.* Antibodies for Vimentin (ID#sc32322, 1/200), EGFR (ID#sc373746, 1/100; p-EGFR (Tyr 1092) ID#sc377547, 1/100), NF-κB (ID#sc8008, 1/5000; p-NF-κB(Ser 536) ID#sc136548, 1/200), AKT (ID#sc8312, 1/200; p-AKT(Ser 473) ID#sc7985, 1/100), p38 (ID#sc7972, 1/100; p-p38(Tiy182) ID#sc-166182, 1/100), FAK (ID#sc271126, 1/200) and PKCα (ID#sc208, 1/500) were from Santa Cruz Biotechnology (Dallas, TX, USA). Antibodies for E-cadherin (ID#3195, 1/1000) and β-actin (ID#4970, 1/1000) were from Cell Signaling Technology (Danvers, MA, USA). Anti HIC-5 antibody (ID#PA5-28839, 1/3000) and anti p-FAK (Tyr397) (ID#44625G, 1/1000) were from Thermo Scientific (Rockford, IL; EEUU). Anti GPR75 antibody (ID#ab75581, 1/500) was from Abcam (Cambridge; UK), and anti GAPDH antibody (ID#MAB374, 1/1000) from (Merck Millipore, Darmstadt, Germany). Polyclonal anti-rabbit (ID#7074S, 1/5000, Cell Signaling Technology) or anti-mouse (ID#NA931VS, 1/10,000, GE Healthcare, Buckinghamshire, UK; or ID#sc516102, 1/6500, Santa Cruz Biotechnology) antibodies conjugated with horseradish peroxidase (HPR) were used as secondary antibodies, accordingly.

For immunofluorescence assays, rhodamine conjugated phalloidin (#P1951, 1/200, Sigma-Aldrich) or anti α-tubulin (ID#sc58666, 1/200, Santa Cruz Biotechnology) were used. 4′,6′-diamidino-2-phenylindole (DAPI) was from Thermo Fisher Scientific. All the other primary antibodies were the same as mentioned above. An anti-mouse linked to rhodamine (ID# 115-025-072, 1/500) and an-anti rabbit secondary antibody (ID#711-165-152, 1/800) from Jackson Immunoresearch, West Grove, PA, USA were used.

GPR75 gene silencing. Human GPR75 siRNA Gene Silencer (sc-94341), Control siRNAs (sc-37007) and support products for siRNA gene silencers were from Santa Cruz Biotechnology.

2.2. Cell culture.

The androgen-insensitive prostate cancer cell line PC-3 was obtained from the American Type Culture Collection (Manassas, VA, USA). Cells were cultured at 37°C with 5% CO_2 for up to 8 weeks and maintained up to 10 passages. They were routinely maintained in RPMI1640 medium supplemented with fetal bovine serum (FBS) 10%, penicillin 100 IU/mL, streptomycin 100 μg/mL, and amphotericin B 2.5 μg/mL (complete medium). When necessary, cells were serum starved 24 h before the experiment. In each case, control conditions refer to the treatment of cells in the absence of drags with the vehicle used at the highest concentration, which never surpassed 0.1%.

2.3. Transfection with siRNA.

Cells were grown on 6-well plates to 80% confluence and were washed with siRNA transfection medium and incubated with the mixture of GPR75 receptor or Control siRNAs and siRNA transfection reagent following manufacturer's instructions (Santa Cruz). The transfection solutions were replaced with fresh complete medium until 90% confluence.

Cells were placed in serum-free medium and treated with the specified drugs as described below.

2.4. Cell fractionation.

Cells were harvested in lysis buffer (Tris, 10 mM; NaCl, 150 mM; Triton X-100® 1%; EDTA, 1 mM; EGTA, 1 mM; $Na_4P_2O_7 \cdot 10H_2O$, 10 mM; Na_3VO_4, 10 mM; and NaF, 100 mM) supplemented with a mix of protease inhibitors (cOmplete™ Mini EDTA-free, Roche Diagnostics, Mannheim Germany). Whole cell extracts for western blotting were prepared as described previously [13]. For subcellular fractionation, cell lysates were first centrifuged at 4°C for 7 min at 3100 xg. The supernatants were further centrifuged at 100,000 xg for 1 h at 4°C. The supernatant was designated as the cytosolic fraction and the pellet was resuspended in lysis buffer containing 0.1% Triton X-100® (30 min at room temperature) and was designated as the membrane fraction [15]. The Bradford method was used for protein determination.

2.5. Western Blot Assays.

Protein separation and blotting were performed as previously described [13]. Briefly, equal amounts of protein were separated by denaturing SDS-PAGE and transferred to polyvinylidene fluoride (PVDF) microporous membranes (Millipore, Boston, MA). The resulting blots were blocked with 5% nonfat milk in TBS/0.1% Tween (TBS-T) or with blocking buffer (bovine serum albumin (BSA), 0.1%; Tween-20, 0.4%; EDTA, 1mM; in TBS-T) (only when anti-goat antibody was used), or with 3% BSA in TBS-T (only when anti phospho-protein antibody was used). The primary antibodies were diluted in TBS-T, and the blots were incubated with these antibodies overnight at 4°C followed by washing in TBS-T and incubation with HRP-conjugated secondary antibodies for 2 h at room temperature. Membranes were developed using a chemiluminescent reagent (ECL Blotting Detection Kit, GE Healthcare) and exposed to films (CL-XPosure Films®, Thermo Scientific, Rockford, IL; USA). The densitometric analysis was performed with ImageJ 1.51j8.

2.6. Cell Viability assay.

Cell viability was determined by MTT assay. In brief, cells were seeded in a 96-well plate at a density of 2×10^3 cells/well, cultured until the confluence reached about 80% and placed in serum-free medium for 24 h. Cells were further grown in the presence or absence of the indicated concentrations of 20-HETE for 16 h before staining with 5 μL of 3-(4,5-dimethylthiazol-2-yl)-2,5-diphenyltetrazolium bromide (MTT) solutions (5 mg/mL) and incubated for 2 h at 37°C until the formazan crystals formed. Then, dimethylsulfoxide (DMSO) was added and the mixture was agitated at a low speed for 15 min to dissolve the formazan crystals, the absorbance (490 mn) was detected using a microtiter plate reader (Synergy HTX, BioTeK, Winooski, Vermont, USA).

2.7. Scratch wound assay.

Cells (2.5×10^5 cells/well) were grown in 6-well plates with complete medium until confluence and placed in serum-free medium for 24 h, then a wound in the cell monolayer

was performed with a sterile pipette tip. After washing with PBS, RPMI was refreshed, and drags were added. Pictures at initial time and after 16 h of incubation were collected. Image analysis included the assessment of the initial and final areas of the wound using the ImageJ 1.51j8. Results are expressed as percentage of migration according to the formula 100-((final area*100)/initial area). Three wounds were made in each well and 9 to 12 microphotographs were taken for each condition.

2.8. Transwell invasion assay.

In vitro cell invasion assays were performed in 10-mm-diameter and 8-μm pore polycarbonate filter transwell plates. Membranes were precoated with 30 μl of a matrigel solution 1:4 on the upper surface, which formed a reconstituted basement membrane at 37°C. PC-3 cells (2×10^5), wild type or GPR75 siRNA- transfected were grown for 24 h in serum-free medium before being seeded on the upper well of the chamber. Subsequently, serum-free medium with vehicle, 20-HETE (0.1 nM) or 19-HEDE (5 μM) was added to the upper chamber, while the lower well was filled to the top (800 μL) with complete medium as a chemoattractant. Cells were allowed to migrate for 16 h. The non-migrating cells were then carefully removed from the upper surface of the transwell with a wet cotton swab, and cells were fixed for 10 min in cold 100% methanol and stained for 5 min with crystal violet. Cells that had invaded to the bottom surface of the filter were counted with a Nikon Ti3 inverted microscope at 40x magnification in a blinded manner, counting 10 high-powered fields per sample. The number of invasive cells was normalized to that of control condition and is expressed as a percentage.

2.9. Soft agar colony formation assay.

A thin layer of agar (0.6%) was placed in 60mm culture plates for 1 h at room temperature. Then, an agar solution (0.35%) containing 5×10^3 cells in the presence or absence of the indicated drugs was laid on top, and plates were left in the incubator for 14 or 21 days. All colonies having more than ten cells were counted using a Nikon Ti3 inverted microscope at low magnification. Results are expressed as Colony Forming Units every 5000 cells.

2.10. Zymography assay.

Cells were grown to confluence in 6-well plates. After washing with PBS, cells were placed in serum-free medium for 24 h in the presence or absence of drugs. Supernatants were collected for zymography assay and the cellular monolayer for total protein assessment. Zymography assay was performed as previously described [16].

2.11. Immunofluorescence assay.

Cells were seeded onto glass coverslips in 24-well plates and allowed to reach 40-60% confluence; then they were washed with PBS before serum deprivation, and were further incubated with 20-HETE in the presence or absence of AAA, or with HET0016 (without serum deprivation) for the indicated times. Cells were washed with PBS, fixed with paraformaldehyde 4% in PBS for 10 min at room temperature, and permeabilized with Triton X-100” 0.2% in PBS for another 10 min. After rinsing with PBS, cells were blocked with BSA 3% in PBS for 1 h. Incubation with phalloidin or specific primary antibodies was

performed for 16 h at 4°C. After rinsing with PBS, samples were incubated with the secondary antibody and DAPI, and mounted. Cells were observed in an Olympus FLUOVIEW FV1000 confocal laser scanning microscope (Olympus Corporation, Tokyo, Japan) and analyzed using the ImageJ 1.51j8 software. Intracellular protein distribution was calculated.

2.12. Statistical Analysis

The statistical analyses were carried out using one-way ANOVA followed by Tukey (multiple comparisons) or Student's t test (two comparisons). Statistics were evaluated using GraphPad Prism V7.0 software (GraphPad Software, La Jolla, CA, USA). Differences were considered significant when $p<0.05$. All results are presented as mean±SEM.

3 RESULTS

3.1 Role of the GPR75 receptor in the intracellular signaling triggered by 20-HETE in androgen-insensitive prostate cancer cells.

The expression of GPR75 receptor protein was firstly confirmed in PC-3 cells cultured in complete or serum-deprived medium. Although the receptor was detected in both conditions, 24 h serum starvation increased GPR75 protein abundance by 91% ($p<0.05$ vs. complete medium) (Fig 1a). Because some GPCRs are internalized and delivered to lysosomes for degradation upon activation [17], we explored the effect of 20-HETE on the expression of the GPR75 receptor. Incubation with 20-HETE (0.1 nM, 12 h) decreased GPR75 receptor abundance in cell homogenates by 78% ($p<0.0001$ vs. control), an effect that was reversed by the 20-HETE receptor antagonist AAA (5 μM) ($p<0.01$ vs. 20-HETE alone). Moreover, AAA increased the expression of GPR75 receptor by 34% ($p<0.01$ vs. control) (Fig 1b).

To investigate the role of the GPR75 receptor in the signaling cascade triggered by 20-HETE in PC-3 cells, changes in intracellular pathways were analyzed in cells treated with 20-HETE in the presence or absence of the GPR75 receptor antagonist.

In human endothelial cells, the GPR75 receptor is associated with Hydrogen Peroxide (H_2O_2) Inducible Clone-5 (Hic-5) [3]. Hic-5 is a 55-kDa inducible focal adhesion protein belonging to the family of paxillin proteins that was identified as a critical modulator of tumor cell phenotype [18], 20-HETE (12 h) dose-dependently increased the expression of HIC-5 up to 95% from 0.01 nM to 1 nM (Fig 2a). The extent of this response was similar to the one of Transforming Growth Factor-betal (TGF-β, 5 and 10 ng/ml) ($p<0.0001$ vs. control for both) (Fig S1a). Incubation with 20-HETE (0.1 nM, 12 h) resulted in a 150% increase in HIC-5 abundance in whole cell homogenates ($p<0.0001$ vs. control). The presence of AAA in the incubation medium completely abolished the effect of 20-HETE ($p<0.0001$ vs. 20-HETE alone for AAA 5 and 10 μM) (Fig 2b).

Protein phosphorylation studies were next performed by using antibodies raised against the phosphorylated or total forms of proteins from the main oncogenic pathways already identified to be activated by 20-HETE. Exposure of PC-3 cells to 20-HETE (0.1nM, 2 h) increased phosphorylation of EGFR, NF-κB and AKT in whole cell homogenates by 146, 172 and 219% respectively (vs. control, $p<0.01$ for NF-κB, and $p<0.001$ for EGFR and

AKT) without modifying protein abundance. The magnitude of the increase in protein phosphorylation elicited by 20-HETE was in the range of the effect of other well-established activators of protein phosphorylation (Fig S1b). Coincubation with the GPR75 receptor antagonist AAA (5 or 10 μM) significantly decreased 20-HETE induced protein phosphorylation (AAA 10 μM, $p<0.05$ for NF-κB, $p<0.01$ for AKT and $p<0.001$ for EGFR, respectively, vs. 20-HETE alone). Conversely, incubation with AAA (10 μM), but not with 20-HETE, increased the phosphorylation of p38 mitogen-activated protein kinase (p38) by 248% ($p<0.0001$ vs. control) and this effect was reversed by the presence of 20-HETE. Moreover, AAA (5 and 10 μM) dose dependently increased p38 phosphorylation even in the presence of 20-HETE ($p<0.001$ and $p<0.0001$ vs. 20-HETE alone for 5 and 10 μM, respectively) (Fig 3).

The effect of 20-HETE (0.1 nM) on the intracellular distribution of total and phospho-AKT, NF-κB and PKCα was further studied. Although intracellular location of total AKT was not altered by 20-HETE, a decrease in its nuclear expression was observed following incubation with AAA ($p<0.01$ vs. control) (Fig 4a). Moreover, an increase in phospho-AKT was observed in cell nuclei in the presence of 20-HETE ($p<0.001$ vs. control), and tins effect was softened by AAA 5 μM ($p<0.01$ vs. 20-HETE alone). Also, AAA induced a significant decrease in the phospho-AKT signal in cell nuclei ($p<0.001$ vs. control) (Fig 4b). Similarly, incubation with AAA mitigated the NF-κB signal that was detected in the nuclei under unstimulated condition ($p<0.001$ vs. control), thus, suggesting that a sustained GPR75 receptor stimulation facilitates NF-κB nuclear location (Fig 4c). On the contrary, for PKCα, incubation with 20-HETE induced a significant withdrawal of protein from the nuclei ($p<0.05$ vs. control) that was not affected by AAA (Fig 4d). Moreover, although non-quantifiable under our experimental imaging conditions, the shift in PKCα signal towards the plasma membrane observed after a 10 min incubation with 20-HETE prompted us to evaluate PKCα intracellular redistribution through subcellular fractionation. Indeed, translocation of PKCα to the plasma membrane is associated with enzyme activation [15]. Under control conditions, a significant amount of PKCα was localized in the cytoplasmic fraction. Ten minutes after treatment with 20-HETE, PKCα was partially re-localized to the cell membrane fraction ($p<0.01$ vs. control). Pretreatment with AAA diminished the membrane associated signal intensity ($p< 0.05$ vs. 20-HETE alone) (Fig 4e).

3.2 20-HETE increases metastatic features of PC-3 cells.

3.2.1 20-HETE promotes a mesenchymal phenotype in PC-3 cells.—

The effect of 20-HETE on the expression level of EMT-associated proteins was first analyzed. The expression of both E-cadherin and vimentin was modified in a concentration dependent manner by 24 h incubation with 20-HETE (0.01 and 0.1 nM). 20-HETE (0.1 nM) was the lowest concentration that significantly decreased the expression of E-cadherin together with a concomitant increase in the expression of vimentin ($p<0.01$ for both) (Fig S2a). The magnitude of the effect of 20-HETE 0.1 nM was similar to the one of the classical inducer of EMT, TGF-β (Fig S2b). The contribution of GPR75 receptor to this effect was further analyzed. 20-HETE (0.1 nM) increased by almost 150% the expression of the mesenchymal marker vimentin ($p<0.0001$ vs. control). This effect was decreased 75% by coincubation with AAA (5 μM) and was abrogated by a higher level of AAA (10 μM) ($p<0.001$ and

p<0.0001 vs. 20-HETE respectively). Correspondingly, the expression of the epithelial marker E-cadherin was downregulated by 40% following incubation with 20-HETE (p<0.0001 vs. control), and this response was reversed by coincubation with AAA (5 or 10 μM) (p<0.05 vs. 20-HETE for both) (Fig 5a). The role of endogenous 20-HETE in promoting EMT was also confirmed since the inhibition of the synthesis of 20-HETE by HET0016 (10 μM, 24h) increased by 71% the expression of E-cadherin and decreased by 73% the expression of vimentin (p<0.05 and p<0.01 vs. control for E-cadherin and vimentin respectively) (Fig 5b).

3.2.2 20-HETE increases motility of PC-3 cells.—The effect of 20-HETE on the migratory capacity of PC-3 cells was assessed by the wound healing assay. Under control conditions, 16 h after the wound was made, the percentage of wound closure was 33.1±2.4%. 20-HETE (0.1-10 nM) increased wound healing, requiring a threshold concentration of 0.1 nM for a significant effect (45.5±1.5% of wound closure, p<0.01 vs. control), that was similar for higher concentrations (Fig S3a). In no case did 20-HETE affect cell viability (Fig S3b). The role of GPR75 receptor in the effect of 20-HETE on cell migration was assessed by cell coincubation with 20-HETE (0.1 nM) and AAA (5 μM). GPR75 receptor antagonism significantly reduced 20-HETE-induced cell migration (% wound closure: 20-HETE, 48.9±2.7%, p<0.0001 vs. control; 20-HETE+AAA, 36.0±2.9, p<0.05 vs. 20-HETE), suggesting that 20-HETE-stimulated cell migration is GPR75-dependent (Fig 6a). Likewise, 19-HEDE amide (19-HEDE, 10 μM), another GPR75 receptor antagonist, impaired 20-HETE-induced cell migration (p<0.0001 vs. 20-HETE). Moreover, 19-HEDE reduced the percentage of wound closure by 20% under control conditions (p<0.01 vs. control) (Fig 6b).

To further asses the role of GPR75 receptor in cell migration promoted by 20-HETE, we used a genetic approach to inhibit GPR75 receptor expression by performing knockdown of the receptor. PC-3 cells were transiently transfected with siRNA against GPR75 receptor (siGPR75) or with a non-targeting siRNA (siControl). The assessment of the knockdown efficiency of GPR75 was confirmed by a decrease of about 40% in the expression of GPR75 protein in cell homogenates (Fig S4). As expected, incubation with 20-HETE (0.1 nM, 16 h) increased wound healing by about 40% in siControl cells (p<0.0001 vs. siControl). Knockdown of GPR75 completely impaired the stimulatory effect of 20-HETE on cell migration (p<0.0001 vs. siControl+20-HETE) (Fig 6c). In line with these findings, the inhibition of the synthesis of 20-HETE by HET0016 significantly reduced wound healing (control 37.9±2.0%; HET0016 1 μM, 30.8±1.7; HET0016 10 μM, 25.5±1.3; p<0.05 and p<0.0001 vs. control respectively) (Fig 6d).

The role of the intracellular pathways activated by 20-HETE (Figs 3–4) on 20-HETE-mediated metastatic features was further investigated on cell migration. Coincubation of 20-HETE with inhibitors of these pathways: PKC (RO318220, 100 nM) (Fig 7a), PI3K/AKT (LY 294002, 25 μM) (Fig 7b) and NF-κB (sulfasalazine, 500 μM) (Fig 7c), significantly reduced 20-HETE-induced cell migration (% wound closure: 20-HETE, 54.2±8.5%, p<0.001 vs. control; 20-HETE+ RO31820, 37.3±10.6, p<0.001 vs. 20-HETE alone; 20-HETE+ LY 294002, 33.0±9.3, p<0.0001 vs. 20-HETE alone; 20-HETE+sulfasalazine, 24.8±7.5, p<0.0001 vs. 20-HETE alone). Moreover, inhibition of PI3K/AKT and NF-κB

decreased cell migration *per se* ($p<0.01$ and $p<0.0001$ vs. control for LY 294002 and sulfasalazine, respectively), thus strengthening the contribution of these pathways to cell migration (Fig 7). These results confirm that the 20-HETE-activated pathways identified in the present study play a critical role in 20-HETE-promoted cell migration.

For cancer cells to invade efficiently, cell motility has to be accompanied by an increase in the ability to degrade the basal membrane. This step is achieved by the release of matrix metalloproteases, such as matrix metalloproteinase-2 (MMP-2). Incubation with 20-HETE (0.1 nM) for 24 h increased MMP-2 activity in PC-3 conditioned medium by 52%, measured as the ability of conditioned medium to hydrolyze collagen (zymography assay) ($p<0.05$ vs. control). Likewise, TGF-β (5 and 10 ng/ml), increased MMP-2 activity by 97% ($p<0.01$ vs. control for both concentrations) (Fig S2c). The role of GPR75 in the increase of MMP-2 activity was confirmed since the response to 20-HETE was abolished by AAA (5 and 10 μM) ($p<0.01$ and $p<0.001$ vs. 20-HETE for AAA at 5 and 10 μM, respectively) (Fig 8a). The involvement of endogenous 20-HETE in MMP-2 activity was further confirmed since the inhibition of the synthesis of 20-HETE by HET0016 (10 μM, 24h) decreased proteolytic activity by 34% ($p<0.01$ vs. control) (Fig 8b).

To elucidate the role of 20-HETE/GPR75 on cell invasiveness, the effect of 20-HETE on transwell invasion was analyzed on wild type PC-3 cells treated with 19-HEDE, and on siControl or siGPR75 PC-3 cells (Fig 9). 20-HETE (0.1 nM, 16 h) increased by 150-200% the invasion capacity in both, wild type and siControl cells ($p<0.0001$ vs. control for both). This effect was reduced by 32% by 19-HEDE in wild type cells ($p<0.0001$ vs. 20-HETE) (Fig 9a). As expected, 20-HETE did not modify invasion when tested on siGPR75 cells ($p<0.0001$ vs. siControl+20-HETE) (Fig 9b). These results confirm the role of GPR75 in 20-HETE-driven invasiveness.

3.2.3 20-HETE contributes to the regulation of actin polymerization in PC-3 cells.—Given that the alterations of cell migration might be related to a destabilization or alterations in the dynamics of cell cytoskeleton, the effect of 20-HETE on α-tubulin or F-actin polymerization was next studied. In control cells, α-tubulin appeared as a filamentous network through the cell cytoplasm, and this disposition was not altered by 24 h incubation with 20-HETE, AAA or HET0016. F-actin in turn was labeled with rhodamine conjugated phalloidin in cells incubated under the same conditions. Control cells predominantly displayed fibrillar structures lying across the cells, with enriched phalloidin labeling at the cell periphery where the F-actin formed membrane protrusions. 20-HETE (0.1 nM) increased the actin stress fibers compared to the control, whereas AAA (10 μM) preserved enriched labeling at cell periphery although it did not allow the correct polymerization of actin filaments (Fig 10a). Consistently, HET0016-treated cells showed a loss of phalloidin staining, suggesting the depolymerization of the actin cytoskeleton (Fig 10b).

Focal adhesion kinase (FAK) is primary implicated in the regulation of signals that mediate cell adhesion to the extra-cellular matrix as well as in the actin cytoskeleton reorganization and cell polarization and, thereby, in cell migration and invasion. Phosphorylation at Tyr397 (Y397) is its major activation mechanism [19]. Western blot analysis of cell lysates showed that incubation with 20-HETE (0.1 nM, 24 h) increased FAK Y397 phosphorylation by 89%

together with a 71% increase in the expression of total FAK ($p<0.0001$ vs control for both). Interestingly, coincubation with AAA 10 μM decreased 20-HETE-induced FAK phosphorylation by 65% ($p<0.001$ vs. 20-HETE) without altering total FAK expression (Fig 10c).

3.2.4 20-HETE increases the ability of PC-3 cells to form colonies in soft agar.—

In vitro anchorage-independent growth, which is defined as the ability of transformed cells to grow independently of a solid surface, is an indication of the metastatic potency of tumors [20].

Cells were plated onto soft agar plates in the presence of the stable synthetic analog of 20-HETE, *N*-(20-hydroxyeicosa-5[Z],14[Z]-dienoyl)glycine (5,14-HEDGE) with or without the addition of AAA or 19-HEDE, or in the presence of HET0016, and allowed to form colonies for fourteen or twenty one days. Cells grown in the presence of 5,14-HEDGE (0.1 nM, 21 days), formed around twice the number of colonies when compared to control cells, and this increase was abolished by coincubation with AAA or 19-HEDE (5 μM for both, $p<0.05$ and $p<0.0001$ vs. 5,14-HEDGE alone respectively), while neither AAA nor 19-HEDE altered the number of colonies *per se*. Correspondingly, a 45% decrease in colony number was observed when HET0016 (10 μM, 14 days) was added to the soft agar medium ($p<0.01$ vs. control) (Fig 11).

4 DISCUSSION

Results from the present study support the importance of GPR75-mediated 20-HETE effects in endowing prostate cancer cells with an aggressive behavior. Indeed, 20-HETE activated intracellular pathways involved in cell transformation lead to an overall enhancement of malignant properties of PC-3 cells. Furthermore, inhibition of the GPR75 receptor, through either a pharmacological or a genetic approach, reduced the pro-tumorigenic effects of 20-HETE in PC-3 cells.

The concentration of 20-HETE used in the present study (0.1 nM) proved to be the lowest one that produced significant effects in our preliminary experiments and is within the range of the calculated Kd for the binding of 20-HETE to GPR75 receptors (3.75 nmol/L) [3]. Moreover, in previous studies from other authors, the same concentration of 20-HETE significantly increased phosphorylation of IkBα and ERK1/2 MAP kinase in endothelial cells [21]. Although it seems to be far below the intracellular 20-HETE levels measured in PC-3 cells (207.3±9.0 ng/mg protein) [13], it should be born in mind that this latter value represents the total endogenous 20-HETE intracellular pool (free plus esterified). Indeed, once produced, 20-HETE can remain unbound to lipids, or can be re-esterified into phospholipids generating a membrane pool of preformed 20-HETE, that constitutes a significant cell reservoir [22].

It is well accepted that the desensitization and downregulation of agonist-occupied GPCRs are primarily mediated by G protein-coupled receptor kinases (GRKs) [23]. GRKs are a family of serine/threonine kinases that are primarily localized to the cytosol and plasma membrane. Upon ligand binding, GRKs phosphorylate serine and threonine residues within

the intracellular carboxy-terminal domain of the receptors. The phosphorylated GPCRs can be then recognized by β-arrestins that bind to the cytosolic surfaces of receptors. As a consequence, β-arrestins can act as scaffolds or adaptors for the binding of other proteins, such as clathrin and clathrin adaptor proteins [24]. Clathrin recruitment and polymerization results in the invagination of the membrane. The ensuing clathrin-coated vesicles or endosomes contain the desensitized GPCR, and these vesicles or endosomes can then fuse to lysosomes for degradation of the receptors, thereby desensitizing cells to further ligand stimulation [17, 25].

In our hands, exposure to 20-HETE for twelve hours decreased expression of the GPR75 receptor. Thus, the resultant decrease in receptor density will prevent the cell from over-responding to the ligand. This response may be understood as a defensive mechanism against the hyperactivation of these receptors that may result in abnormally amplified signals throughout the cell leading to aberrant cell physiological properties. On the other hand, overexpression of the GPR75 receptor in serum starving cells may be viewed as an adaptive response when the enviromnent is depleted of other growth factors.

GPCR signaling generally results in the transmission of amplified signals throughout the cell, and hyperactivation of these receptors may result in abnormal cell behavior. Indeed, GPCRs play integral roles in regulating and activating cancer-associated signaling pathways, and can induce signaling cascades as well as downstream kinases such as phosphoinositide 3-kinase (PI3K)/AKT and MAPK pathways [27]. Furthermore, depending on the receptor and cell type, GPCRs signaling involves transactivation of several different receptor tyrosine kinases (RTKs), such as EGFR and receptor serine/threonine kinases [28]. In line, the present results show that the 20-HETE-mediated activation of EGFR, NF-κB, AKT and PKCα previously described in other cells [6, 15, 29] requires stimulation from the GPR75 receptor. Conversely, phosphorylation of p38, even if not affected by 20-HETE, was triggered by the antagonism of GPR75. This observation should be interpreted with the knowledge that activation of p38 signaling exerts tumor suppressive functions on metastatic cells by causing growth arrest, senescence or apoptosis [30, 31].

One of the ultimate goals of cellular signaling is the control of gene expression in the nucleus. In our hands, the 20-HETE driven increase of p-AKT in the nucleus together with the withdrawal of NF-κB elicited by AAA raises the hypothesis that 20-HETE may transmit signals into the nucleus in a GPR75-dependent manner. Indeed, the increased nuclear localization of signaling molecules has been previously reported in some kinds of cancer. Despite its increased nuclear expression in cancer cells, AKT has been shown to migrate into the nucleus in response to a wide variety of stimuli that include insulin-like growth factor-1 (IGF-1), hypoglycemia, insulin, and nerve growth factor (NGF). Indeed, some of AKT substrates are resident in the nucleus, such as the FOXO family of transcription factors or the transcriptional co-activator p300 [32]. Moreover, the presence of active, phosphorylated AKT within the nucleus has been described in prostate cancer [33]. Our results suggest that a sustained GPR75 receptor stimulation facilitates AKT and NF-κB nuclear location, whereas an increase in 20-HETE signaling induces nuclear AKT phosphorylation.

The contribution of three of the pathways assessed in this study (PI3K/AKT, NF-κB, and PKC) to the 20-HETE-stimulated malignant cell features was confirmed by the observation that selective inhibitors of these pathways decreased the effect of 20-HETE on cell migration.

The oncogenic role of the PI3K/AKT axis on tumor growth extends beyond its pro-proliferative and survival effects and includes migration and invasion [34]. AKT-mediated phosphorylation of the EMT transcription factor TWIST1 promotes EMT and breast cancer metastasis [35]. NF-κB contributes to cancer formation and invasiveness as a result of its specific transcriptional activity [36]. Among other tumors, activation of NF-κB was probed to be essential for EMT and metastasis in a model of breast cancer progression [37] and promoted the growth of prostate cancer cells in bone [38]. PKCα in its turn, is overexpressed in prostate cancer [39], and its activation resulted in increased cell motility associated with increased invasiveness in several *in vivo* and *in vitro* cancer models [40]. Thus, as a common driver of various oncogenic signaling pathway in prostate cancer cells, targeting 20-HETE/GPR75 might be considered an attractive target for the development of anticancer agents.

Besides the canonical GPCRs-associated signal transducers mentioned above, in the present study we present evidence that 20-HETE increases total cellular levels of Hic-5 in a GPR75-dependent manner. Hic-5 is involved in transcriptional regulation as well as in cytoskeletal organization, contractile activity, and cell spreading [41]. More recently, Hic-5 overexpression in tumor cell lines proved to be sufficient to drive a shift toward a mesenchymal morphology and to promote phenotypic plasticity and invasion [18]. A recent publication confirmed that transcriptional activation of Hic-5 is positively regulated by NADPH oxidase-ROS-c-Jun N-terminal kinase (JNK) pathway and found one putative binding motif for c-jun, the downstream transcriptional factor of ROS-JNK pathway, in the binding regions on Hic-5 promoter responsible for activation of Hic-5 gene [42]. Interestingly, a number of reports have described that 20-HETE increases NADPH oxidase-derived ROS production in normal and tumor tissues [43, 44, 7]; and increases JNK phosphorylation, thus interfering with the c-Jun pathway in gliosarcoma cells [45]. Therefore, although other pathways should not be ruled out, we hypothesize that the increase in HIC-5 expression elicited by 20-HETE might be related to its well-known capacity of stimulating ROS production.

Epithelial-mesenchymal transition allows a polarized epithelial cell to undergo multiple biochemical changes that enable it to assume a mesenchymal phenotype, which includes activation of transcription factors, expression of specific cell-surface proteins, reorganization and expression of cytoskeletal proteins, production of extracellular matrix-degrading enzymes, degradation of underlying basement membrane, and the formation of a mesenchymal cell that can migrate away from the epithelial layer in which it originated [46]. The observation that the expression of both protein markers for EMT (vimentin and E-cadherin) were altered by incubation with HET0016 or with 20-HETE, and that the latter response was abolished by the antagonism of its receptor, strongly suggests that 20-HETE induces EMT through GPR75 receptor stimulation. Also, inhibition of the synthesis of 20-HETE, or GPR75 knockdown and/or pharmacological antagonism abrogated cell migration,

secretion of MMP-2 into the conditioned medium and invasiveness capacity. These results support a role for 20-HETE/GPR75 in these well-known key components for tumor metastasis.

Cell migration is a dynamic process that requires the coordinated rearrangement of the cytoskeleton and cell adhesion. Our results support a role for endogenously synthetized 20-HETE and for the GPR75 receptor in the regulation of the structure of the actin cytoskeleton as well as the phosphorylation of FAK. However, the fact that 20-HETE-induced expression of total FAK was not affected by AAA, suggests that this mechanism is GPR75-independent. Other authors have shown that cytoskeletal reorganization caused by the binding of ligands to actin allows not only the inhibition of migration, but also apoptosis of cancer cells [47, 48]. Therefore, given its role in cellular transformation and biologic processes, disruption of the actin cytoskeleton has been proposed as a potential antitumoral therapeutic target [49, 50].

Finally, our results from the *in vitro* assay for colony formation in soft agar suggest that the 20-HETE/GPR75 pathway plays a pivotal role in metastasis of prostate cancer cells via regulating anoikis resistance and anchorage-independent growth. While these *in vitro* results are encouraging, *in vivo* studies are needed for confirmation of the role of 20-HETE in promoting prostate cancer metastasis.

Most prostate tumors initially shrink in response to androgen-deprivation therapy [14], but ultimately progress to the castration-resistant metastatic form. Management of castration resistant prostate cancer is a clinical challenge. Therefore, there is a need for developing drugs with novel mechanisms of action and different mechanisms of resistance compared to the classical antiandrogens [51]. Previous studies have demonstrated increased expression levels of the secreted form of phospholipase A_2 (sPLA2-IIA) that mediates the release of AA in patients with prostate cancer [52]. Moreover, the specific up-regulation of $sPLA_2$-IIA in the highest-grade prostate cancer samples highlights the importance of AA metabolites for tumor progression [53]. Our present results provide evidence supporting the hypothesis that inhibition of the synthesis of 20-HETE or the antagonism of GPR75 receptor are antitumoral approaches that might be considered promising for further evaluation in the management of the castration resistant prostate cancer in the future.

Supplementary Material

Refer to Web version on PubMed Central for supplementary material.

Acknowledgments:

This work was supported by grant 1006/2016 from the National Cancer Institute (INC-Argentina) to SN, grant 11220150100118CO from the Argentinean National Research Council (CONICET) to MC and SN. JRF was supported by the Robert A. Welch Foundation (I-0011) and NIH HL139793.

Abbreviations:

5, 14-HEDGE	N-(20-hydroxyeicosa-5[Z],14[Z]-dienoyl)glycine

19-HEDE amide	sodium 19(R)-hydroxyeicosa-5(Z), 14(Z)-dienoyl-L-aspartate
20-HETE	20-hydroxyeicosatetraenoic acid
AA	Arachidonic acid
AAA	Sodium ((6Z,15Z)-N-(20-hydroxyeicosa-6(Z),15(Z)-dienoyl)aspartate)
AKT	Protein Kinase B
COX	Cyclooxygenase
CRPC	Castration-resistant prostate cancer
CYP	Cytochrome P450
DAPI	4′,6′-diamidino-2-phenylindole
DMSO	Dimethylsulfoxide
EGFR	Epidermal growth factor receptor
EMT	Epithelial-mesenchymal transition
FAK	Focal adhesion kinase
GPCR	G-protein coupled receptor
GRKs	G protein-coupled receptor kinases
HET0016	hydroxy-N′-(4-n-butyl-2-methylphenyl)formamidine
HIC-5	Hydrogen Peroxide Inducible Clone-5
HPR	Horseradish peroxidase
IGF-1	Insulin-like growth factor-1
LOXs	Lipoxygenase
MAPK	Mitogen-activated protein kinases
MMP-2	Metalloproteinase-2
MTT	3-(4,5-dimethylthiazol-2-yl)-2,5-diphenyltetrazolium bromide
NF-κB	Nuclear factor-κB
PI3K	Phosphoinositide 3-kinase
PLC	Phospholipase C
PKC	Protein kinase C

RTKs	Receptor tyrosine kinases
sPLA2	Secreted form of phospholipase A2
TGF-β	Transforming Growth Factor-beta1
TNF-α	Tumor Necrosis Factor-alpha

REFERENCES

1. Powell PK, Wolf I, Jin R, Lasker JM, Metabolism of arachidonic acid to 20-hydroxy-5,8,11,14-eicosatetraenoic acid by P450 enzymes in human liver: involvement of CYP4F2 and CYP4A11., J. Pharmacol. Exp. Ther, 285, 1327–1336, (1998). [PubMed: 9618440]
2. Fan F, Roman RJ, GPR75 Identified as the First 20-HETE Receptor: A Chemokine Receptor Adopted by a New Family., Circ. Res, 120, 1696–1698, (2017), DOI: 10.1161/CIRCRESAHA.117.311022. [PubMed: 28546348]
3. Garcia V, Gilani A, Shkolnik B, Pandey V, Zhang FF, Dakarapu R, Gandham SK, Reddy NR, Graves JP, Gruzdev A, Zeldin DC, Capdevila JH, Falck JR, Schwartzman ML, 20-HETE Signals Through G Protein-Coupled Receptor GPR75 (Gq) to Affect Vascular Function and Trigger Hypertension, Circ. Res, 120, 1776–1788, (2017), DOI: 10.1161/CIRCRESAHA.116.310525. [PubMed: 28325781]
4. Sauer CG, White K, Stöhr H, Grimm T, Hutchinson A, Bernstein PS, Lewis RA, Simonelli F, Pauleikhoff D, Allikmets R, Weber BH, Evaluation of the G protein coupled receptor-75 (GPR75) in age related macular degeneration., Br. J. Ophthalmol, 85, 969–975, (2001), DOI: 10.1136/bjo.85.8.969. [PubMed: 11466257]
5. Alexanian A, Rufanova V. a., Miller B, Flasch A, Roman RJ, Sorokin A, Down-regulation of 20-HETE synthesis and signaling inhibits renal adenocarcinoma cell proliferation and tumor growth. Anticancer Res., 29, 3819–3824, (2009). [PubMed: 19846914]
6. Shankar A, Borin TF, Iskander A, Varma NR, Achyut BR, Jain M, Mikkelsen T, Guo AM, Chwang WB, Ewing JR, Bagher-Ebadian H, Arbab AS, Combination of vatalanib and a 20-HETE synl Shankar A, Borin TF, Iskander A, Varma NR, Achyut BR, Jain M, Mikkelsen T, Guo AM, Chwang WB, Ewing JR, Bagher-Ebadian H, Arbab AS, Combination of vatalanib and a 20-HETE synthesis inh, Onco. Targets. Ther, 9, 1205–1219, (2016), DOI: 10.2147/OTT.S93790. [PubMed: 27022280]
7. Guo AM, Sheng J, Scicli GM, Arbab AS, Lehman NL, a Edwards P, Falck JR, Roman RJ, Scicli a G., Expression of CYP4A1 in U251 human glioma cell induces hyperproliferative phenotype in vitro and rapidly growing tumors in vivo., J. Pharmacol. Exp. Ther, 327, 10–19, (2008), DOI: 10.1124/jpet.108.140889\rjpet.108.140889. 108.140889 [pii]. [PubMed: 18591218]
8. Yu W, Chen L, Yang Y-Q, Falck JR, Guo AM, Li Y, Yang J, Cytochrome P450 ω-hydroxylase promotes angiogenesis and metastasis by upregulation of VEGF and MMP-9 in non-small cell lung cancer., Cancer Chemother. Pharmacol, 68, 619–629, (2011), DOI: 10.1007/s00280-010-1521-8. [PubMed: 21120482]
9. Borin TF, Angara K, Rashid MH, Achyut BR, Arbab AS, Arachidonic Acid Metabolite as a Novel Therapeutic Target in Breast Cancer Metastasis., Int. J. Mol. Sci, 18, (2017), DOI: 10.3390/ijmsl8122661.
10. Rieger MA, Ebner R, Bell DR, Kiessling A, Rohayem J, Schmitz M, Tetmne A, Rieber EP, Weigle B, Identification of a Novel Matmnary-Restricted Cytochrome P450, CYP4Z1, with Overexpression in Breast Carcinoma, Cancer Res., 64, 2357–2364, (2004), DOI: 10.1158/0008-5472.CAN-03-0849. [PubMed: 15059886]
11. Tradonsky A, Rubin T, Beck R, Ring B, Seitz R, Mair S, A Search for Reliable Molecular Markers of Prognosis in Prostate Cancer, Am. J. Clin. Pathol, 137, 918–930, (2012), DOI: 10.1309/AJCPF3QWIG8FWXIH. [PubMed: 22586051]
12. Nithipatikom K, Isbell MA, See WA, Campbell WB, Elevated 12- and 20-hydroxyeicosatetraenoic acid in urine of patients with prostatic diseases., Cancer Lett., 233, 219–225, (2006), DOI: 10.1016/j.canlet.2005.03.025. [PubMed: 15882928]

13. Colombero C, Papademetrio D, Sacca P, Monnandi E, Alvarez E, Nowicki S, Role of 20-Hydroxyeicosatetraenoic Acid (20-HETE) in Androgen-Mediated Cell Viability in Prostate Cancer Cells, Horm. Cancer, 8, 243–256, (2017), DOI: 10.1007/s12672-017-0299-0. [PubMed: 28639228]
14. Huggins C, V Hodges C, Studies on Prostatic Cancer: I. The Effect of Castration, of Estrogen and of Androgen Injection on Serum Phosphatases in Metastatic Carcinoma of the Prostate, J. Urol, 168, 9–12, (2006), DOI: 10.1016/s0022-5347(05)64820-3.
15. Nowicki S, Kruse MS, Brismar H, Aperia A, Dopamine-induced translocation of protein kinase C isoforms visualized in renal epithelial cells. Am. J. Physiol. Cell Physiol, 279, 0812–0818, (2000), DOI: 10.1152/ajpcell.2000.279.6.C1812.
16. Soares Machado M, Rosa FD, Lira MC, Urtreger AJ, Rubio MF, Costas MA, The inflammatory cytokine TNF contributes with RAC3-induced malignant transformation, EXCLI J., 17, 1030–1042, (2018), DOI: 10.17179/EXCLI2018-1759. [PubMed: 30585274]
17. Lefkowitz RJ, Rajagopal K, Whalen EJ, New roles for beta-arrestins in cell signaling: not just for seven-transmembrane receptors., Mol. Cell, 24, 643–652, (2006), DOI: 10.1016/j.molcel.2006.11.007. [PubMed: 17157248]
18. Gulvady AC, Dubois F, Dcakin NO. Goreczny GJ, Turner CE, Hic-5 expression is a major indicator of cancer cell morphology, migration, and plasticity in three-dimensional matrices. Mol. Biol. Cell, 29, 1704–1717, (2018), DOI: 10.1091/mbc.E18-02-0092. [PubMed: 29771639]
19. Mousson A. Sick E, Carl P, Dujardin D, De Mey J, Ronde P, Targeting Focal Adhesion Kinase Using Inhibitors of Protein-Protein Interactions, Cancers (Basel)., 10, 278, (2018), DOI: 10.3390/cancers10090278.
20. Mori S, Chang JT, Andrechek ER, Matsumura N, Baba T, Yao G, Kim JW, Gatza M, Murphy S, Nevins JR, Anchorage-independent cell growth signature identifies tumors with metastatic potential. Oncogene, 28, 2796–805, (2009), DOI: 10.1038/onc.2009.139. [PubMed: 19483725]
21. Ishizuka T, Cheng J, Singh H, Vitto MD, Manthati VL, Falck JR, Laniado-schwartzman M, 20-Hydroxyeicosatetraenoic Acid Stimulates Nuclear Factor- B Activation and the Production of Inflammatory Cytokines in Human Endothelial Cells, 324, 103–110, (2008), DOI: 10.1124/jpet.107.130336.tion.
22. Carroll MA, Balazy M, Huang DD, Rybalova S, Falck JR, Mcgiff JC, Cytochrome P450-derived renal HETEs: Storage and release. Kidney Int, 51, 1696–1702, (1997), DOI: 10.1038/ki.1997.234. [PubMed: 9186856]
23. Pfleger J, Gresham K, Koch WJ, G protein-coupled receptor kinases as therapeutic targets in the heart, Nat. Rev. Cardiol, (2019), DOI: 10.1038/s41569-019-0220-3.
24. Krupnick JG, Goodman OB, Keen JH, Benovic JL, Arrestin/clathrin interaction. Localization of the clathrin binding domain of nonvisual arrestins to the carboxy terminus., J. Biol. Chem, 272, 15011–6, (1997), DOI: 10.1074/jbc.272.23.15011. [PubMed: 9169476]
25. Baugher PJ, Richmond A, The carboxyl-terminal PDZ ligand motif of chemokine receptor CXCR2 modulates post-endocytic sorting and cellular chemotaxis., J. Biol. Chem, 283, 30868–78, (2008), DOI: 10.1074/jbc.M804054200. [PubMed: 18755694]
26. Lefkowitz RJ, Shenoy SK, Transduction of receptor signals by beta-arrestins., Science, 308, 512–517, (2005), DOI: 10.1126/science.1109237. [PubMed: 15845844]
27. Yu S, Sun L. Jiao Y, Lee LTO, The Role of G Protein-coupled Receptor Kinases in Cancer., Int. J. Biol. Sci, 14, 189–203, (2018), DOI: 10.7150/ijbs.22896. [PubMed: 29483837]
28. Xia S, He C, Zhu Y, Wang S, Li H, Zhang Z, Jiang X, Liu J, GABABR-Induced EGFR Transactivation Promotes Migration of Human Prostate Cancer Cells., Mol. Pharmacol, 92, 265–277, (2017), DOI: 10.1124/mol.116.107854. [PubMed: 28424220]
29. Garcia V, Brian S. Milhau L, Falck JJ, Sclnvartzman M. 20-HETE Activates the Transcription of Angiotensin Converting Enzyme (ACE) via NF-kB Translocation and Promoter Binding., J. Pharmacol. Exp. Ther, 525–533, (2015), DOI: 10.1124/jpet.115.229377. [PubMed: 26699146]
30. V Bulavin D, Fomace AJ, p38 MAP kinase's emerging role as a tumor suppressor., Adv. Cancer Res, 92, 95–118, (2004), DOI: 10.1016/S0065-230X(04)92005-2. [PubMed: 15530558]
31. Aguirre-Ghiso JA, Models, mechanisms and clinical evidence for cancer donnancy, Nat. Rev. Cancer, 7, 834–846, (2007), DOI: 10.1038/nrc2256. [PubMed: 17957189]

32. Martelli AM, Tabellini G, Bressanin D, Ognibene A, Goto K, Cocco L, Evangelisti C, The emerging multiple roles of nuclear Akt, Biochim. Biophys. Acta - Mol. Cell Res, 1823, 2168–2178, (2012), DOI: 10.1016/j.bbamcr.2012.08.017.
33. Van de Sande T, Roskams T, Lerut E, Joniau S, VanPoppel H, Verhoeven G, V Swinncn J. High-level expression of fatty acid synthase in human prostate cancer tissues is linked to activation and nuclear localization of Akt/PKB, J. Pathol, 206, 214–219, (2005), DOI: 10.1002/path.1760. [PubMed: 15880754]
34. Porta C, Paglino C, Mosca A, Targeting PI3K/Akt/mTOR Signaling in Cancer., Front. Oncol, 4, 64, (2014), DOI: 10.3389/fonc.2014.00064. [PubMed: 24782981]
35. Xue G, Restuccia DF, Lan Q, Hynx D, Dirnhofer S, Hess D, Riiegg C, Hemmings BA, Akt/PKB-mediated phosphorylation of Twistl promotes tumor metastasis via mediating crosstalk between PI3K/Akt and TGF-β signaling axes., Cancer Discov., 2, 248–59, (2012), DOI: 10.1158/2159-8290.CD-11-0270. [PubMed: 22585995]
36. Kaltschmidt B, Greiner JFW, Kadhim HM, Kaltschmidt C, Subunit-Specific Role of NF-κB in Cancer., Biomedicines, 6, (2018), DOI: 10.3390/biomedicines6020044.
37. Huber MA, Azoitei N, Baumann B, Griinert S, Soimner A, Pehamberger H, Kraut N, Beug H, Wirth T, NF-kappaB is essential for epithelial-mesenchymal transition and metastasis in a model of breast cancer progression., J. Clin. Invest, 114, 569–81, (2004), DOI: 10.1172/JCI21358. [PubMed: 15314694]
38. Jin R, Sterling JA, Edwards JR, DeGraff DJ, Lee C, Park SI, Matusik RJ, Activation of NF-kappa B Signaling Promotes Growth of Prostate Cancer Cells in Bone, PLoS One, 8, e60983, (2013), DOI: 10.1371/journal.pone.0060983. [PubMed: 23577181]
39. Koren R, Meir D, Langzam L, Dekel Y, Konichezky M, Baniel J, Livne P, Gal R, Sampson S, Expression of protein kinase C isoenzymes in benign hyperplasia and carcinoma of prostate, Oncol. Rep, 11, 321–326, (2004), DOI: 10.3892/or.11.2.321. [PubMed: 14719062]
40. Martiny-Baron G, Fabbro D, Classical PKC isoforms in cancer, Pharmacol. Res, 55, 477–486, (2007), DOI: 10.1016/j.phrs.2007.04.001. [PubMed: 17548205]
41. Shibanuma M, Mori K, Nose K, HIC-5: A mobile molecular scaffold regulating the anchorage dependence of cell growth, Int. J. Cell Biol, 2012, 1–8, (2012), DOI: 10.1155/2012/426138.
42. Wu J-R, You R-I, Hu C-T, Cheng C-C, Rudy R, Wu W-S, Hydrogen peroxide inducible clone-5 sustains NADPH oxidase-dependent reactive oxygen species-c-jun N-terminal kinase signaling in hepatocellular carcinoma. Oncogenesis, 8, 40, (2019), DOI: 10.1038/s41389-019-0149-8. [PubMed: 31387985]
43. Zeng Q, Han Y, Bao Y, Li W, Li X, Shen X, Wang X, Yao F, O'Rourke ST, Sun C, 20-HETE increases NADPH oxidase-derived ROS production and stimulates the L-type Ca2+ channel via a PKC-dependent mechanism in cardiomyocytes., Am. J. Physiol. Heart Circ. Physiol, 299, H1109–17, (2010), DOI: 10.1152/ajpheart.00067.2010. [PubMed: 20675568]
44. Han Y, Zhao H, Tang H, Li X, Tan J. Zeng Q, Sun C, 20-Hydroxyeicosatetraenoic acid mediates isolated heart ischemia/reperfusion injury by increasing NADPH oxidase-derived reactive oxygen species production, Circ. J, 77, 1807–1816, (2013), DOI: 10.1253/circj.CJ-12-1211. [PubMed: 23585488]
45. Guo M, Roman RJ, Fenstennacher JD, Brown SL, Falck JR, Arbab AS, Edwards PA, Scicli AG, 9L gliosarcoma cell proliferation and tumor growth in rats are suppressed by N-hydroxy-N'-(4-butyl-2-methylphenol) formamidine (HET0016), a selective inhibitor of CYP4A., J. Pharmacol. Exp. Ther, 317, 97–108, (2006), DOI: 10.1124/jpet.105.097782. [PubMed: 16352703]
46. Kalluri R, Weinberg RA, The basics of epithelial-mesenchymal transition., J. Clin. Invest, 119, 1420–1428, (2009), DOI: 10.1172/JCI39104. [PubMed: 19487818]
47. Pawlik A, Szczepanski MA, Klimaszewska A, Gackowska L, Zuryn A, Grzanka A, Phenethyl isothiocyanate-induced cytoskeletal changes and cell death in lung cancer cells., Food Chem. Toxicol, 50, 3577–3594, (2012), DOI: 10.1016/j.fct.2012.07.043. [PubMed: 22847136]
48. Zhou G-Z, Cao F-K, Du S-W, The apoptotic pathways in the curcumin analog MHMD-induced lung cancer cell death and the essential role of actin polymerization during apoptosis., Biomed. Pharmacother, 71, 128–134, (2015), DOI: 10.1016/j.biopha.2015.02.025. [PubMed: 25960227]

49. Budryn G, Grzelczyk J, Perez-Sanchez H, Binding of Red Clover Isoflavones to Actin as A Potential Mechanism of Anti-Metastatic Activity Restricting the Migration of Cancer Cells., Molecules, 23, 2471, (2018), DOI: 10.3390/molecules23102471.

50. Schmidt MCB, Morais KLP, de Almeida MES, Iqbal A, Goldfeder MB, Chudzinski-Tavassi AM, Amblyomin-X, a recombinant Kunitz-type inhibitor, regulates cell adhesion and migration of human tumor cells., Cell Adh. Migr, 1–10, (2018), DOI: 10.1080/19336918.2018.1516982.

51. Ito Y, Sadar MD, Enzalutamide and blocking androgen receptor in advanced prostate cancer: lessons learnt from the history of drag development of antiandrogens., Res. reports Urol, 10, 23–32, (2018), DOI: 10.2147/RRU.S157116.

52. Sved P, Scott KF, Mcleod D, King NJC, Singh J, Tsatralis T, Nikolov B, Boulas J, Nallan L, Gelb MH, Sajinovic M, Graham GG, Russell PJ, Oncogenic Action of Secreted Phospholipase A2 in Prostate Cancer, Cancer Res., 64, 6934–6940, (2006), DOI: 10.1158/0008-5472.CAN-03-3018.

53. Oleksowicz L, Liu Y, Bracken RB. Gaitonde K, Burke B, Succop P, Levin L, Dong Z, Lu, Secretory phospholipase A2-IIa is a target gene of the HER/HER2-elicited pathway and a potential plasma biomarker for poor prognosis of prostate cancer., Prostate, 72, 1140–1149, (2012), DOI: 10.1002/pros.22463. [PubMed: 22127954]

Highlights

- Androgen-insensitive prostate cancer cells (PC-3) express the 20-HETE receptor, GPR75.
- Stimulation of GPR75 by 20-HETE increases metastatic features of PC-3 cells.
- The inhibition of 20-HETE synthesis diminished metastatic features of PC-3 cells.
- 20-HETE-GPR75 triggered signaling pathways involved in cell malignant transformation.

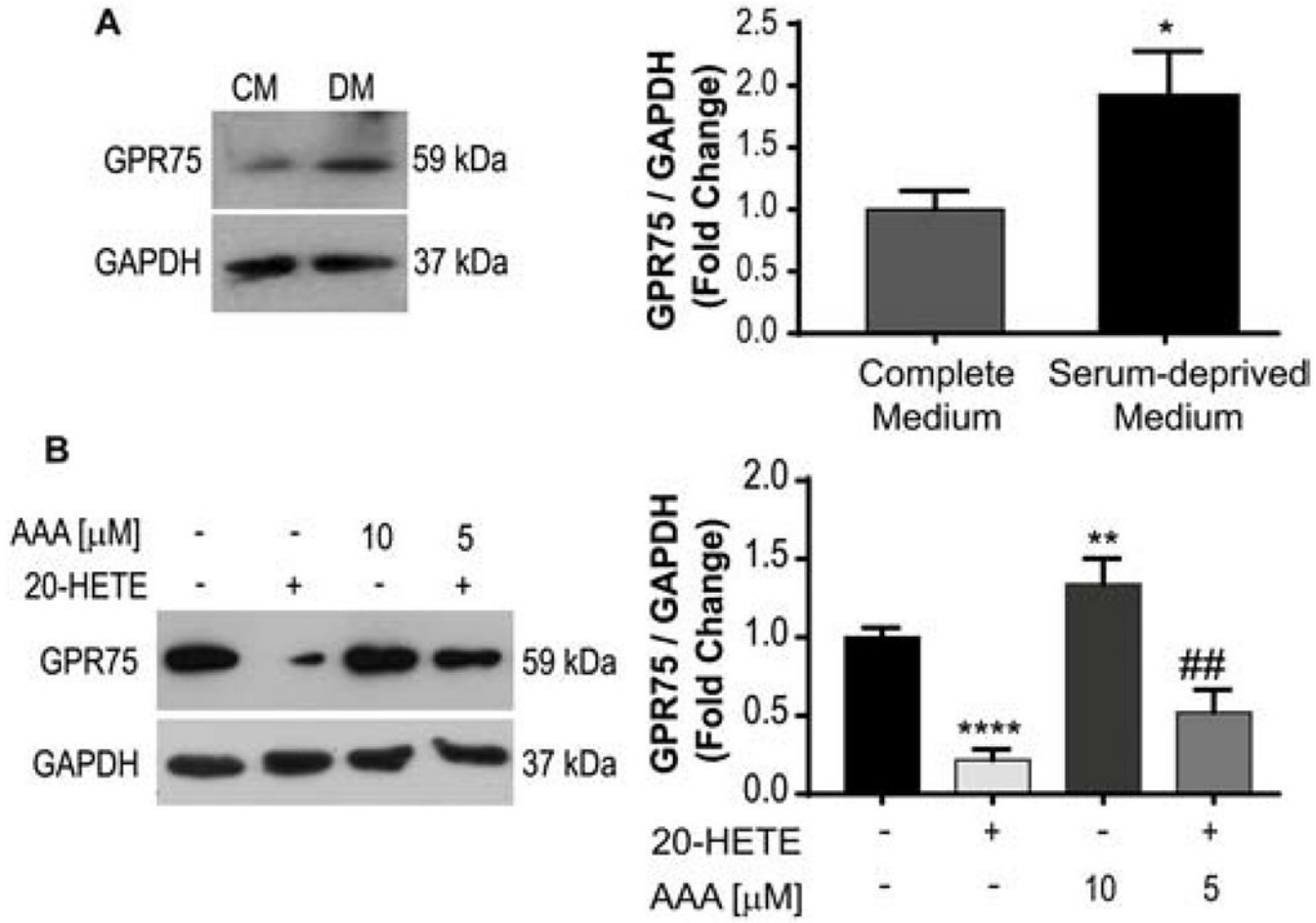

Fig 1. Expression of GPR75 in PC-3 cells.

A. Cells grown in RPMI medium supplemented with fetal bovine serum (10%) (complete medium, CM) (control) or in 24 h-serum deprived medium (DM) (n=3). **B.** Cells grown for 24 h in serum deprived medium in the presence of vehicle only (control), or 20-HETE (0.1 nM, 12 h) with or without the addition of the antagonist sodium ((6Z,15Z)-20-hydroxyeicosa-6,15-dienoyl)aspartate (AAA, 5 or 10 μM) (n=4-5).

A representative western blot of whole cell homogenates is presented. The quantitation of the receptor expression is shown as the ratio GPR75/GAPDH. Densitometry data were normalized to that of control condition and are expressed as the means ± SE. (*p<0.05, **p<0.01, ****p<0.0001 vs. Control; ##p<0.01 vs. 20-HETE alone)

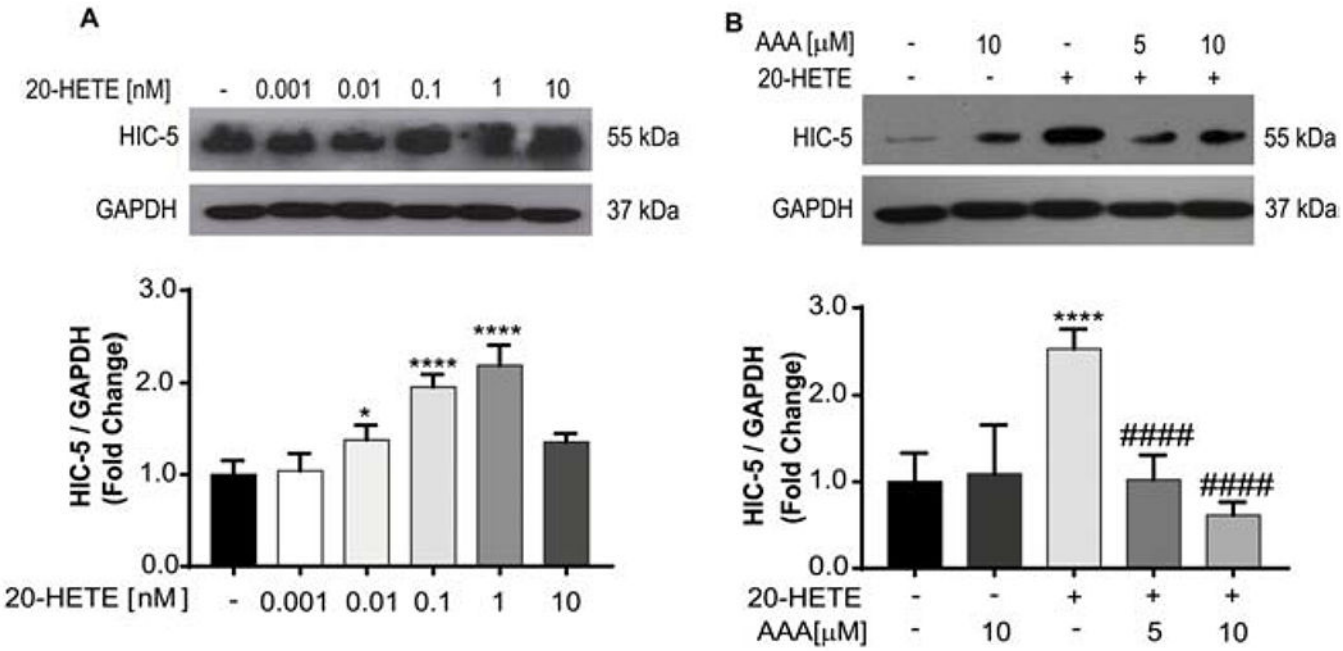

Fig 2. HIC-5 expression in PC-3 cells.

Cells grown for 24 h in serum deprived medium were incubated for 12 h with vehicle only (control) or: **A.** the indicated concentrations of 20-HETE (n=3). **B.** 20-HETE (0.1 nM) in the presence or absence of AAA (5 or 10 μM) (n=5).

A representative western blot of whole cell homogenates is presented. The quantitation of the receptor expression is shown as the ratio HIC-5/GAPDH. Densitometry data were normalized to that of control condition and are expressed as the means ± SE (*p<0.05, ****p<0.0001 vs. Control; ####p<0.0001 vs. 20-HETE alone)

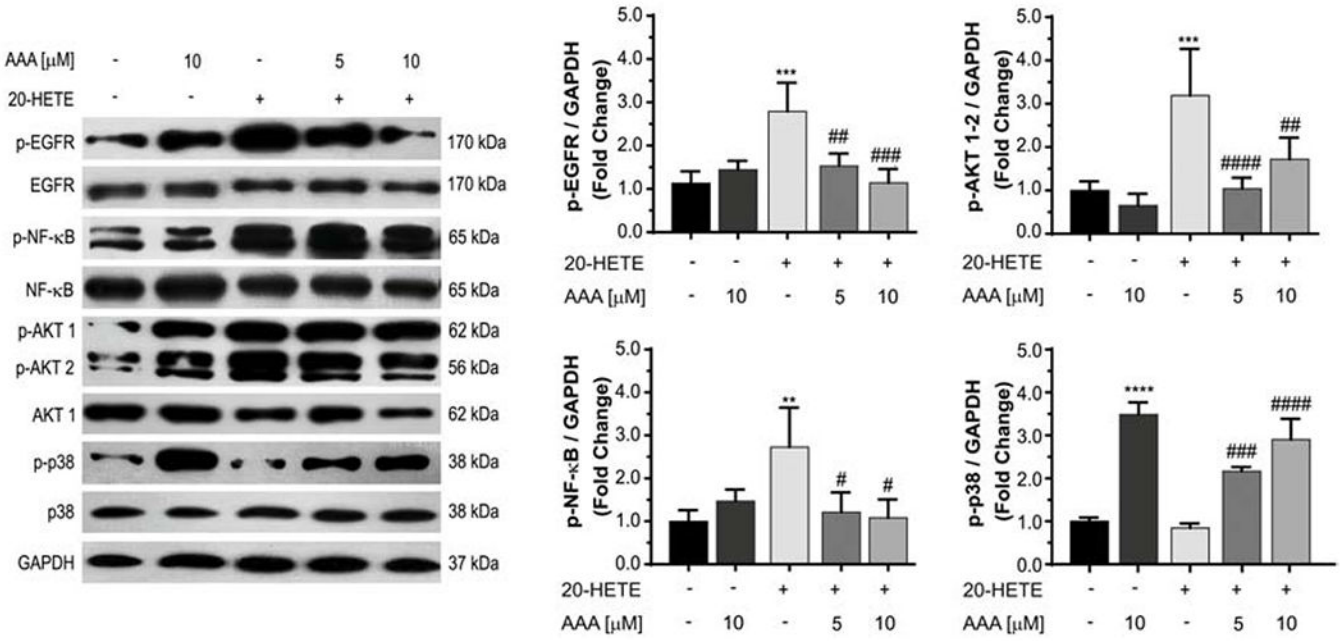

Fig 3. Protein phosphorylation.

Cells grown for 24 h in serum deprived medium were incubated for 2 h with vehicle (control) or 20-HETE (0.1 nM) in the presence or absence of AAA (5 or 10 μM). Phosphospecific antibodies against p-EGFR (Tyr 1092), p-NFκB p65 (Ser 536), p-AKT (p-AKTl and p-AKT2) (Ser 473), p-p38 (Tyr 182) were used. A representative western blot of whole cell homogenates is presented. The quantitation of protein phosphorylation is shown as the ratio p-protein/GAPDH. Densitometry data were normalized to that of control condition, and are expressed as the means ± SE. (n=3-4) (**p<0.01, ***p<0.001, ****p<0.0001 vs. Control; #p<0.05, ##p<0.01, ###p<0.001.####p<0.0001 vs. 20-HETE alone)

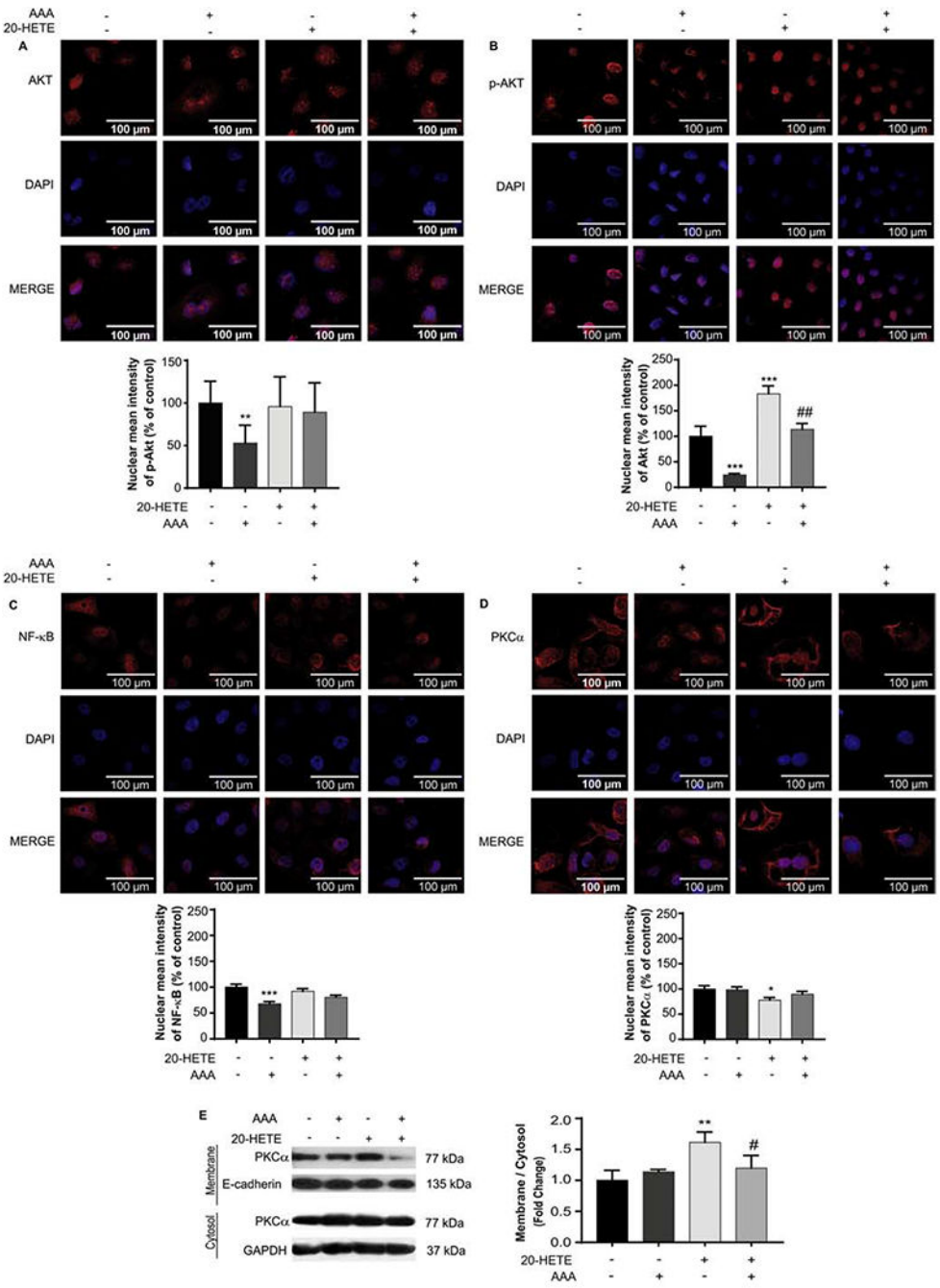

Fig 4. Intracellular protein distribution.

Cells grown for 24 h in serum deprived media were incubated with vehicle only (control) or 20-HETE (0.1 nM) in the presence or absence of AAA (5 μM) for 60 min (total AKT, p-AKT and NF-κB) or 10 min (PKCα) and prepared for immunofluorescence imaging or subjected to subcellular fractionation. **A.-D.** Representative immunofluorescence micrographs and quantification of intracellular distribution of total AKT **(A)**, p-AKT **(B)**, NF-kB **(C)**, or PKCα **(D)** (n=3). **E.** Representative western blot of the expression of PKCα in membrane and cytosolic fractions. The expression of PKCα in membrane and cytosolic

fraction was normalized to the one of E-cadherin and GAPDH, respectively. The quantitation is shown as the ratio between membrane-bound and cytosolic PKCα (n=2). Data were normalized to that of control condition, and are expressed as the means ± SE. (*p<0.05, **p<0.01 ***p<0.001 vs. Control; #p<0.05 ##p<0.01 vs. 20-HETE alone)

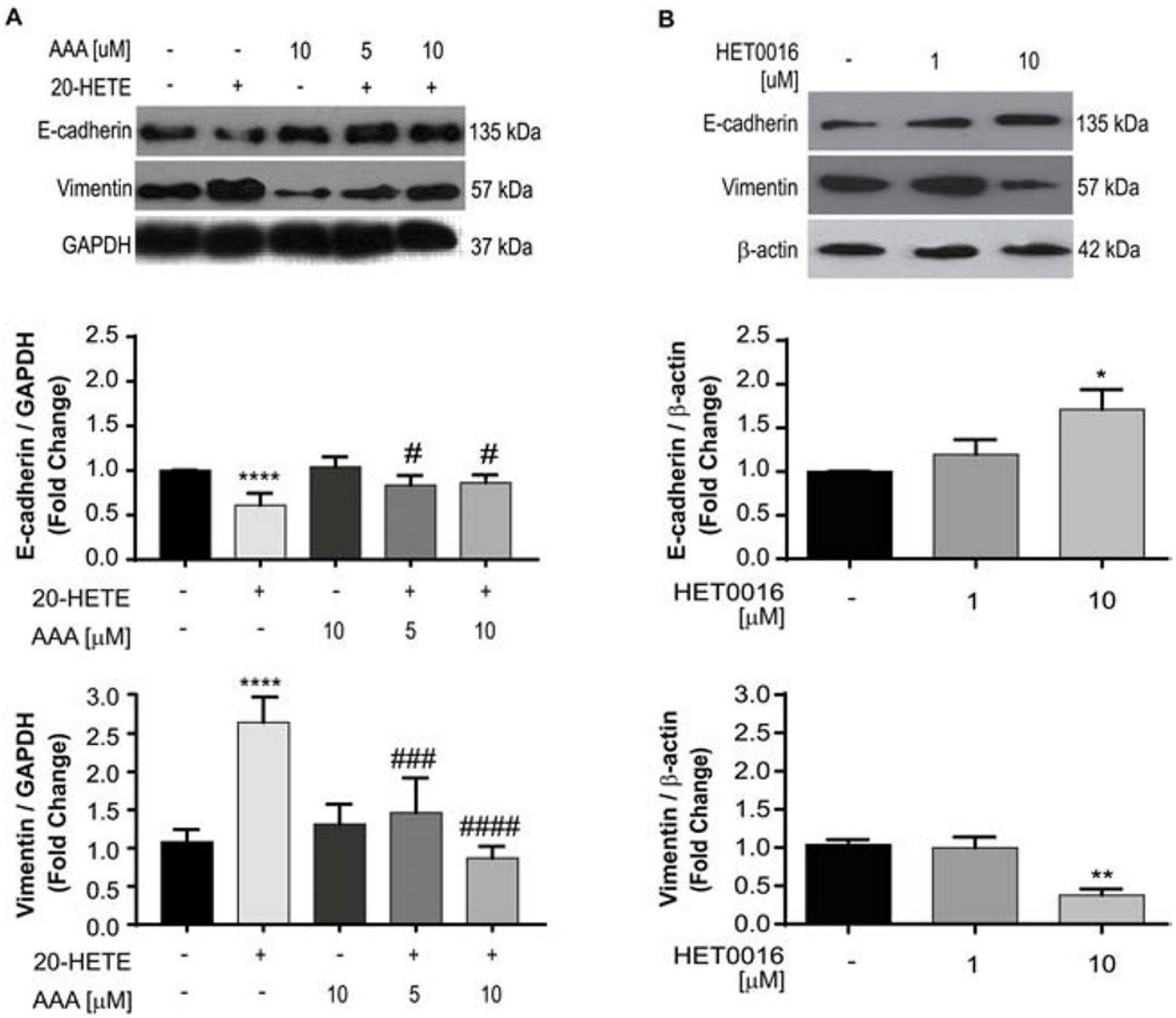

Fig 5. Epithelial-Mesenchymal transition markers.

Cells grown for 24 h in: **A.** serum deprived medium or **B.** complete medium were incubated for 24 h with vehicle only (control) or in the presence of: **A.** 20-HETE (0.1 nM) with or without the addition of AAA (5 or 10 μM) (n=4), or **B.** HET0016 (1 or 10 μM) (n=4). A representative western blot of whole cell homogenates is presented. The quantitation of protein expression is shown as the ratio of Protein/GAPDH or Protein/β-actin. Densitometry data were normalized to that of control condition and are expressed as the means ± SE (*p<0.05, **p<0.01, ****p<0.0001 vs. Control; #p<0.05, ###p<0.001, ####p<0.0001 vs. 20-HETE alone)

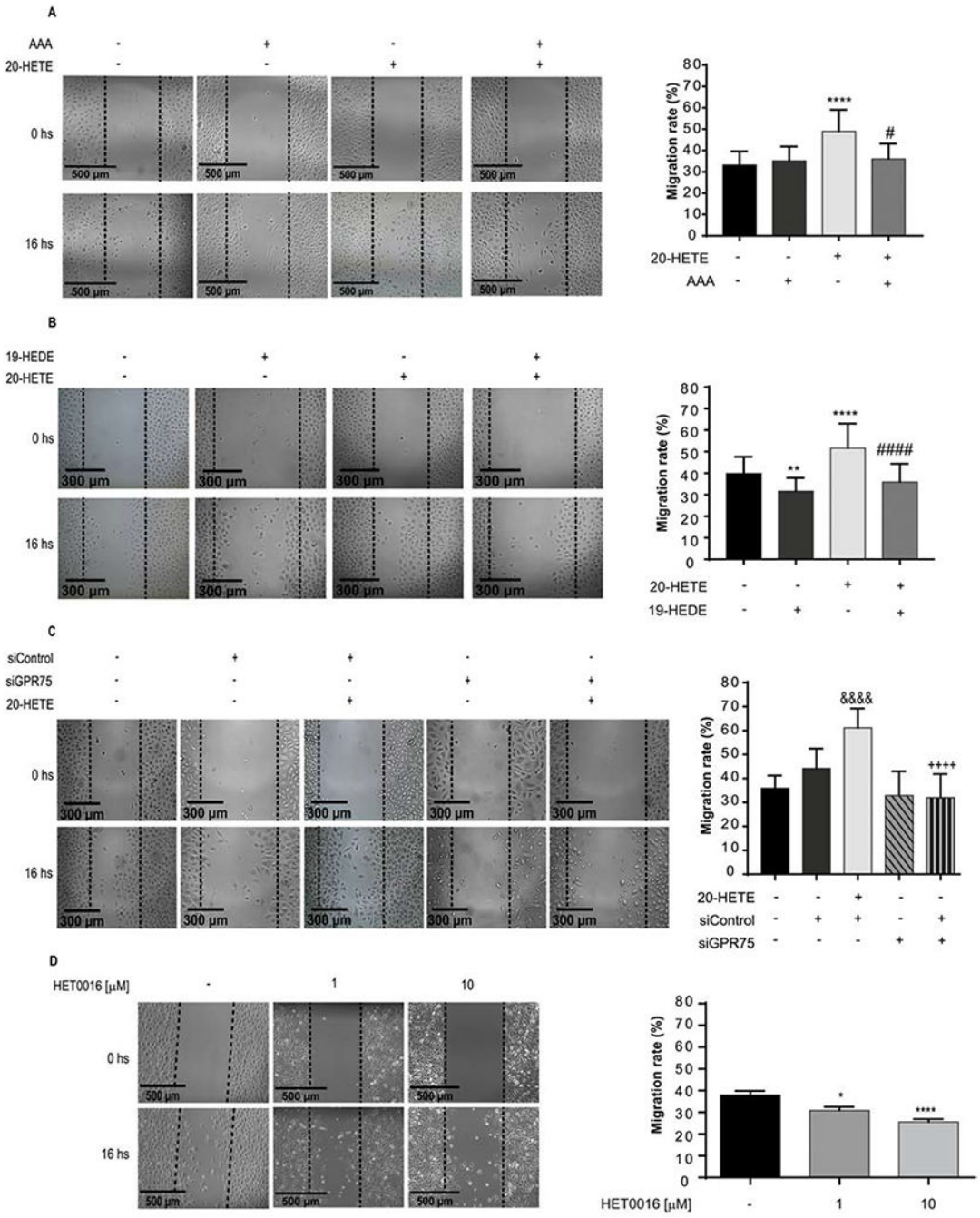

Fig 6. 20-HETE/GPR75 and cell migration.

PC-3 cells were grown up to 90-100% confluency, and were serum deprived for 24 h. After the wound was made, cells were incubated for another 16 h in the presence of vehicle only (control) or the following conditions: 20-HETE (0.1 nM) with or without the addition of the GPR75 antagonists, **A.** AAA (5 μM) (n=3), **B.** Sodimn 19(R)-hydroxyeicosa-5(Z), 14(Z)-dienoyl-L-aspartate (19-HEDE, 5 μM) (n=3). **C.** Wild type cells (control) or cells transfected with control siRNA (siControl) or GPR75 siRNA (siGPR75) incubated with 20-HETE (0.1 nM) (n=3). **D.** HET0016 (1 or 10 μM) (n=2-4)

Images were acquired at 0 and 16 h. Representative wound assay brightfield images are shown. The dotted lines define the areas lacking cells. Quantification of wound assay is represented as % migration rate after 16 h compared to a 0 h control (9-12 photographs per condition were analyzed). Values are presented as the mean± SEM. (*p<0.05, **p<0.01, ****p<0.0001 vs. control; #p<0.05, #### p<0.0001 vs. 20-HETE; &&&& p<0.0001 vs. siControl; ++++p<0.0001 vs siControl+20-HETE).

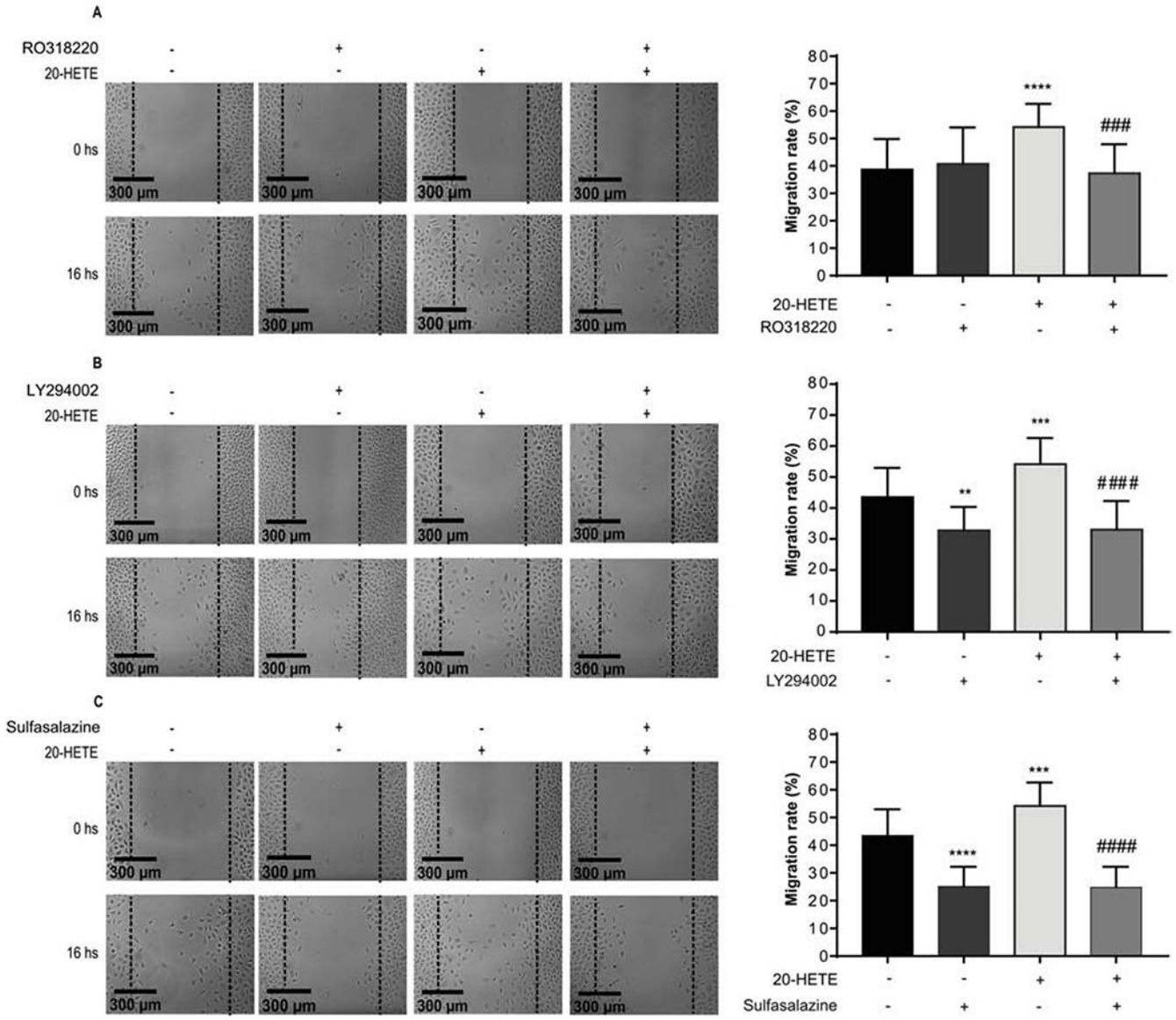

Fig 7. 20-HETE-activated cell pathways and cell migration.

PC-3 cells were grown up to 90-100% confluency, and were serum deprived for 24 h. After the wound was made, cells were incubated for another 16 h in the presence of vehicle only (control) or the following conditions: 20-HETE (0.1 nM) with or without the addition of the following inhibitors: **A.** RO318220 (PKC pathway, 100 μM) (n=3), **B.** LY294002 (PI3K/AKT pathway, 25 μM) (n=3), **C.** sulfasalazine (NF-κB pathway, 500 μM) (n=3). Images were acquired at 0 and 16 h. Representative wound assay brightfield images are shown. The dotted lines define the areas lacking cells. Quantification of wound assay is represented as % migration rate after 16 h compared to a 0 h control (9-12 photographs per condition were analyzed). Values are presented as the mean ± SEM. (**p<0.01, ***p<0.001, ****p<0.0001 vs. control; ###p<0.001, #### p<0.0001 vs. 20-HETE).

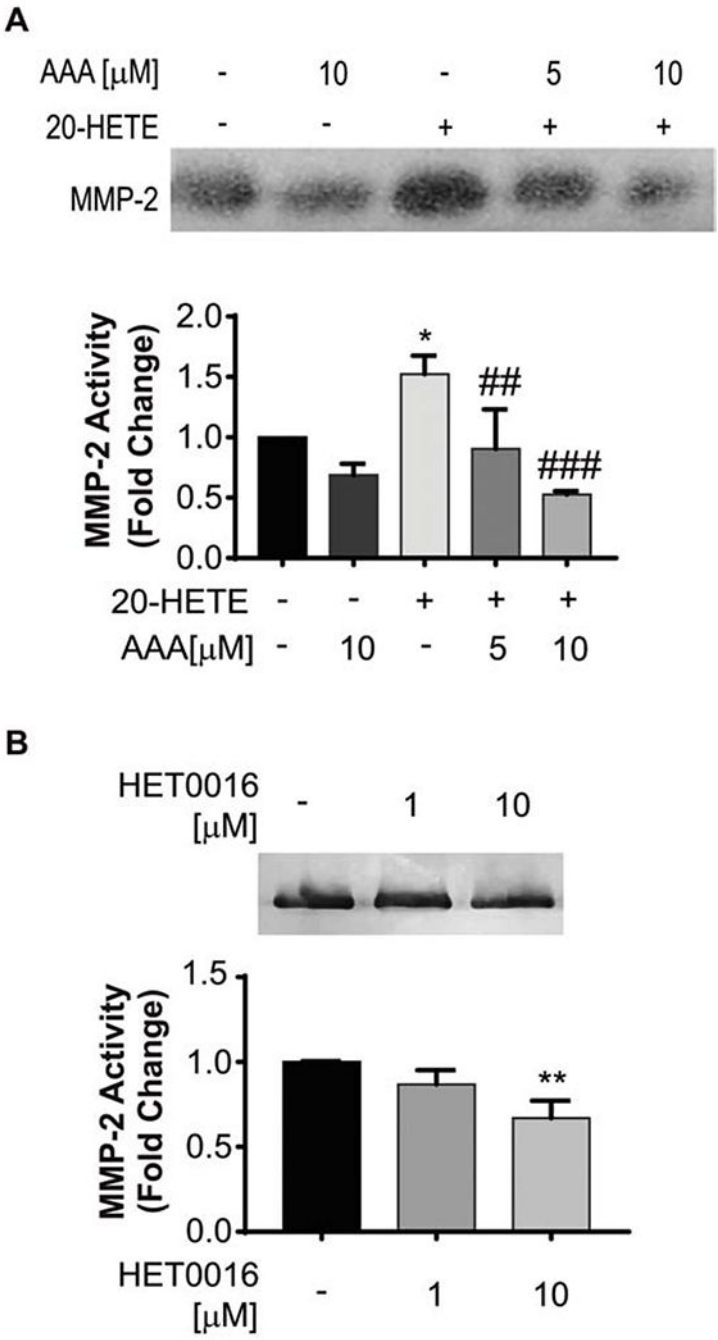

Fig 8. MMP-2 activity.

Cells grown for 24 h in: **A.** serum deprived medium or, **B.** complete medium, were incubated for 24 h with vehicle only (control) or in the presence of: **A.** 20-HETE (0.1 nM) with or without the addition of AAA (5 or 10 μM), or **B.** HET0016 (1 or 10 μM). A representative image of the zymography assay is presented. Quantitative values are presented as fold change of the control condition and are expressed as the means ± SE (n=2 in duplicates). (*p<0.05, **p<0.01 vs. control; ## p<0.01, ###p<0.001 vs. 20-HETE alone).

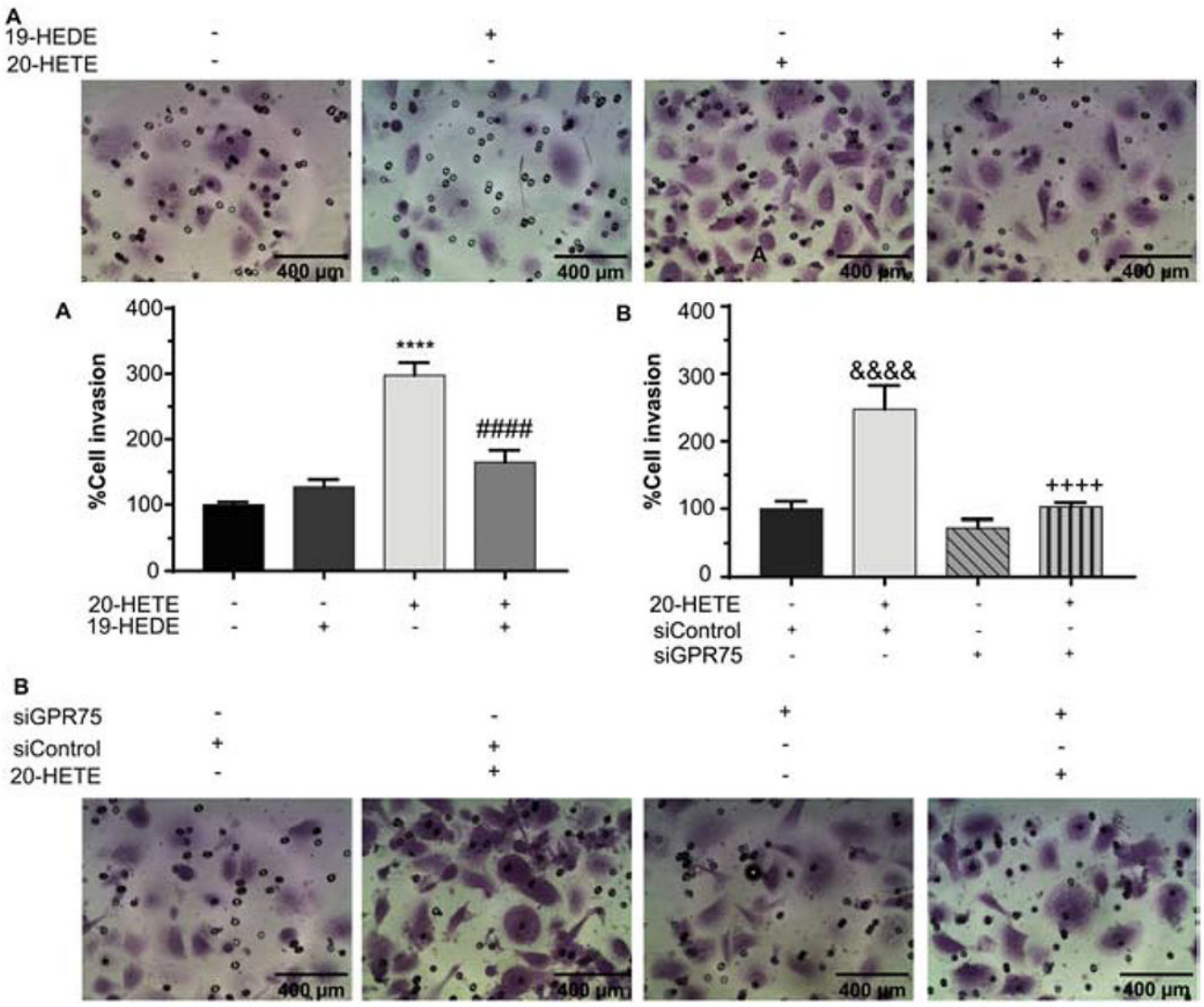

Fig 9. Cell Invasion.

A. Wild type cells or **B.** cells transfected with control siRNA (siControl) or GPR75 siRNA (siGPR75), grown for 24 h in serum free medium, were seeded in serum free medium in the upper chamber of matrigel coated trans-well plates and were incubated with vehicle only (control) or with 20-HETE (0.1 nM) with or without the addition of the GPR75 antagonist 19-HEDE (5 μM) (n=2). After 16 h invasive cells attached to the bottom surface of the membrane were stained and quantified. Representative transwell assay images are shown. The number of invasive cells was normalized to that of control condition and is expressed as a percentage. Values are presented as the means ± SEM. ****$p<0.0001$ vs. control; #### $p<0.0001$ vs. 20-HETE; &&&& $p<0.0001$ vs. siControl; ++++$p<0.0001$ vs siControl+20-HETE).

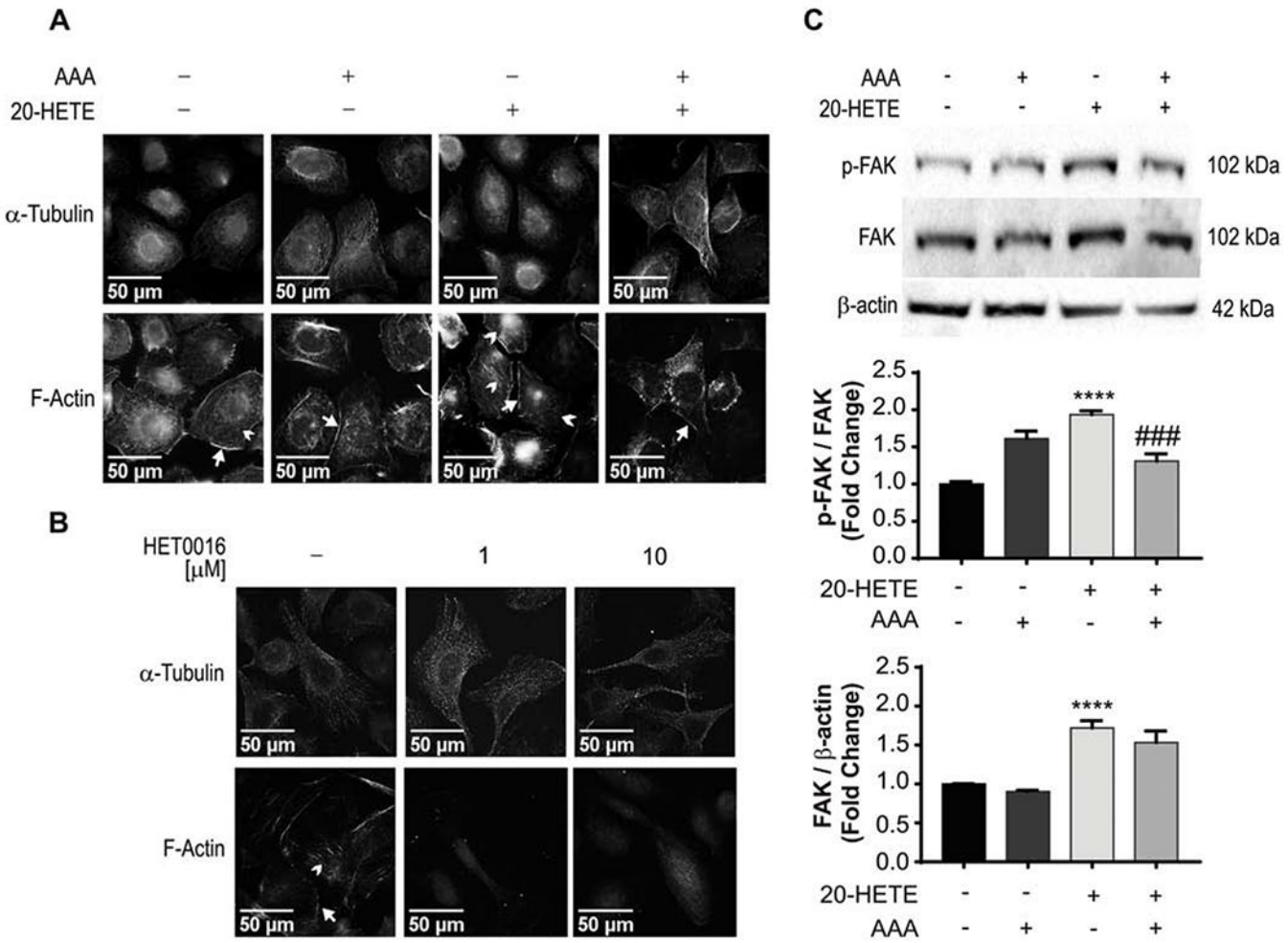

Fig 10. Cell cytoskeleton polymerization.

A. and **C.** PC-3 cells grown for 24 h in serum free medium were further incubated for 24 h with vehicle only (control) or 20-HETE (0.1 nM) in the presence or absence of AAA (10 μM). **B.** PC-3 cells grown in complete medium were incubated for 24 h with vehicle only (control) or HET0016 1 or 10 μM. **A.** and **B.** Representative cell images of α-tubulin (upper panel) or F-actin (lower panel) are presented. Immunofluorescent staining of F-actin with phalloidin was assessed for stress fibers (arrowheads), and focal adhesions (arrows). **C.** Western blot image of the expression of phospho (p-) (Tyr397) or total focal adhesion kinase (FAK) in cell homogenates. The quantitation of FAR phosphorylation is shown as p-FAK/FAK ratio and that of total FAK expression as FAK/β-actin ratio. Densitometry data were normalized to that of the control condition and are expressed as the means ± SE. (****$p<0.0001$ vs control; ###$p<0.001$ vs. 20-HETE alone).

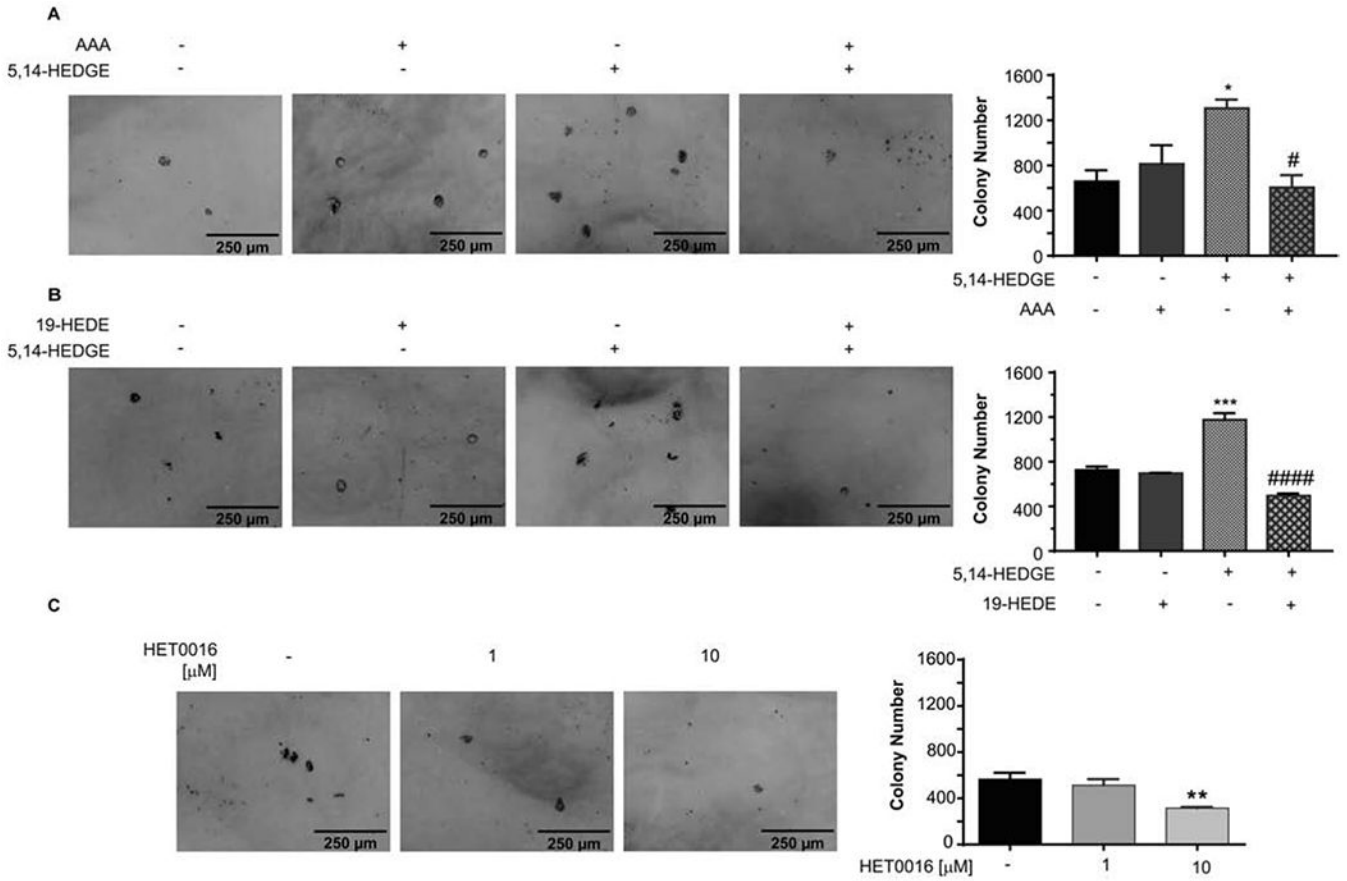

Fig 11. Colony formation in soft agar.

PC-3 cells were plated at a density of 5×10^3 cells/plate and were grown for 21 days in the presence of vehicle only (control) or N-(20-hydroxyeicosa-5[Z],14[Z]-dienoyl)glycine (5,14-HEDGE, 0.1 nM) with or without the addition of the GPR75 antagonists, **A.** AAA (5 µM), **B.** 19-HEDE (5 µM). **C.** Cells were plated in complete media in the presence of vehicle only (control) or HET0016 (1 or 10 µM) and grown for 14 days. Representative brightfield images are shown. Only colonies larger than 10 cells were scored as positive. Quantification of soft agar assay is presented as colony number (n = 2 in duplicates,). Values are presented as the means ± SEM. (*p<0.05, **p<0.01. ***p<0.001 vs. control; #p<0.05, ####p<0.0001 vs. 5,14-HEDGE alone).